

Highly oxygenated organic molecules (HOM) formation in the isoprene oxidation by NO₃ radical

Defeng Zhao^{1, 2, 3, 4}, Iida Pullinen^{2, a}, Hendrik Fuchs², Stephanie Schrade², Rongrong Wu², Ismail-Hakki Acir^{2, b}, Ralf Tillmann², Franz Rohrer², Jürgen Wildt², Yindong Guo¹, Astrid Kiendler-Scharr², Andreas Wahner², Sungah Kang², Luc Vereecken², Thomas F. Mentel²

¹Department of Atmospheric and Oceanic Sciences & Institute of Atmospheric Sciences, Fudan University, Shanghai, 200438, China;

²Institute of Energy and Climate Research, IEK-8: Troposphere, Forschungszentrum Jülich, 52425, Jülich, Germany

³Big Data Institute for Carbon Emission and Environmental Pollution, Fudan University, Shanghai, 200438, China

⁴Institute of Eco-Chongming (IEC), 20 Cuinia Rd., Chenjia Zhen, Chongming, Shanghai 202162, China

^aNow at: Department of Applied Physics, University of Eastern Finland, Kuopio, 7021, Finland.

^bNow at: Institute of Nutrition and Food Sciences, University of Bonn, Bonn, 53115, Germany;

Correspondence to: Thomas F. Mentel (t.mentel@fz-juelich.de), Defeng Zhao (dfzhao@fudan.edu.cn)

Abstract

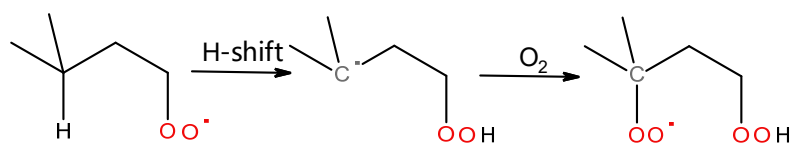
Highly oxygenated organic molecules (HOM) are found to play an important role in the formation and growth of secondary organic aerosol (SOA). SOA is an important type of aerosol with significant impact on air quality and climate. Compared with the oxidation of volatile organic compounds by ozone (O₃) and hydroxyl radical (OH), HOM formation in the oxidation by nitrate radical (NO₃), an important oxidant at night-time and dawn, has received less attention. In this study, HOM formation in the reaction of isoprene with NO₃ was investigated in the SAPHIR chamber (Simulation of Atmospheric PHotochemistry In a large Reaction chamber). A large number of HOM including monomers (C₅), dimers (C₁₀), and trimers (C₁₅), both closed-shell compounds and open-shell peroxy radicals (RO₂), were identified and were classified into various series according to their formula. Their formation pathways were proposed based on the peroxy radicals observed and known mechanisms in the literature, which were further constrained by the time profiles of HOM after sequential isoprene addition to differentiate first- and second-generation products. HOM monomers containing one to three N atoms (1-3N monomers) were formed, starting with NO₃ addition to carbon double bond, forming peroxy radicals, followed by autoxidation. 1N monomers were formed by both the direct reaction of NO₃ with isoprene and of NO₃ with first-generation products. 2N-monomers (e.g. C₅H₈N₂O_n (n=7-13), C₅H₁₀N₂O_n (n=8-14)) were likely the termination products of C₅H₉N₂O_n[•], which was formed by the addition of NO₃ to C5-hydroxynitrate (C₅H₉NO₄), a first-generation product containing one carbon double bond. 2N-monomers, which were second-generation products, dominated in monomers and accounted for ~34% of all HOM, indicating the important role of second-generation oxidation in HOM formation in the isoprene+NO₃ reaction under our experimental conditions. H-shift of alkoxy radicals to form peroxy radicals and subsequent autoxidation (“alkoxy-peroxy” pathway) was found to be an important pathway of HOM formation. HOM dimers were mostly formed by the accretion reaction of various HOM monomer RO₂ and via the termination reactions of dimer RO₂ formed by further reaction of closed-shell dimers with NO₃ and possibly by the reaction of C5-RO₂ with isoprene. HOM trimers were likely formed by the accretion reaction of dimer RO₂ with monomer RO₂. The concentrations of different HOM showed distinct time profiles during the reaction, which was linked to their formation pathway. HOM concentrations either showed a typical time profile of first-generation products, or of second-generation products, or a combination of both, indicating multiple formation pathways and/or multiple isomers. Total HOM molar yield was estimated to be 1.2%^{+1.3%}_{-0.7%}, which corresponded to a SOA yield of ~3.6% assuming the molecular weight of C₅H₉NO₆

41 as the lower limit. This yield suggests that HOM may contribute a significant fraction to SOA yield in the reaction
42 of isoprene with NO_3 .

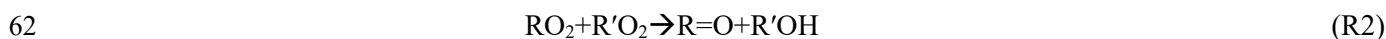
43 1 Introduction

44 Highly oxygenated organic molecules (HOM) are an important class of compounds formed in the oxidation
45 of volatile of organic compounds (VOC) including biogenic VOC (BVOC) and anthropogenic VOC (Crouse
46 et al., 2013; Ehn et al., 2014; Jokinen et al., 2014; Rissanen et al., 2014; Jokinen et al., 2015; Krechmer et al.,
47 2015; Mentel et al., 2015; Rissanen et al., 2015; Kenseth et al., 2018; Molteni et al., 2018; Garmash et al., 2019;
48 McFiggans et al., 2019; Molteni et al., 2019; Quelever et al., 2019). A number of recent studies have
49 demonstrated that HOM play a pivotal role in both nucleation and also particle growth of pre-existing particles,
50 thus contributing to secondary organic aerosol (SOA) (Ehn et al., 2014; Kirkby et al., 2016; Tröstl et al., 2016).
51 Particularly, in the early stage of aerosol growth, HOM may contribute a significant fraction of SOA mass
52 (Tröstl et al., 2016).

53 HOM are formed by the autoxidation of peroxy radicals (RO₂), which means they undergo intramolecular
54 H-shift forming alky radicals, followed by O₂ addition leading to formation of new RO₂ as shown below
55 (Vereecken et al., 2007; Crouse et al., 2013; Ehn et al., 2017; Bianchi et al., 2019; Møller et al., 2019; Nozière
56 and Vereecken, 2019; Vereecken and Nozière, 2020).



58 Besides autoxidation, the RO₂ can also react with HO₂, RO₂ and NO₃, either forming a series of termination
59 products (R1-3), including organic hydroperoxide, alcohol, and carbonyl, or forming alkoxy radicals (RO,
60 R4-5) via the following reactions.



67 The termination products are detected in the mass spectra at masses M+1, M-15, M-17 respectively with
68 M being the molecular mass of the parent RO₂ (Ehn et al., 2014; Mentel et al., 2015). In case that RO₂ is an acyl
69 peroxy radical, percarboxylic acids and carboxylic acids are formed instead of hydroperoxides and alcohols in
70 R3 and R1, respectively (Atkinson et al., 2006; Mentel et al., 2015). RO₂ can also form HOM dimers by the
71 accretion reaction of two RO₂ (R6) (Berndt et al., 2018a; Berndt et al., 2018b; Valiev et al., 2019). Additionally,
72 HOM can be formed via H-shift in RO followed by O₂ addition (referred to as “alkoxy-proxy” pathway)
73 (Finlayson-Pitts and Pitts, 2000; Vereecken and Peeters, 2010; Vereecken and Francisco, 2012; Mentel et al.,
74 2015). These pathways are summarized in a recent comprehensive review (Bianchi et al., 2019), which also
75 further clarifies HOM definition.

76 Currently, most laboratory studies of HOM formation focus on the VOC oxidation by OH and O₃ (Crouse
77 et al., 2013; Ehn et al., 2014; Jokinen et al., 2014; Rissanen et al., 2014; Jokinen et al., 2015; Krechmer et al.,
78 2015; Mentel et al., 2015; Rissanen et al., 2015; Kirkby et al., 2016; Tröstl et al., 2016; Kenseth et al., 2018;
79 Molteni et al., 2018; Garmash et al., 2019; McFiggans et al., 2019; Molteni et al., 2019; Quelever et al., 2019;
80 Wang et al., 2020; Yan et al., 2020). HOM formation in the oxidation of VOC with NO₃ has received much less
81 attention. NO₃ is another important oxidant of VOC mainly operating during nighttime. Particularly, NO₃ has
82 high reactivity with unsaturated BVOC such as monoterpene and isoprene. It is often the dominant oxidant of
83 these compounds at night, especially in regions where biogenic and anthropogenic emissions mix (Geyer et al.,
84 2001; Brown et al., 2009; Brown et al., 2011). The reaction products contribute to SOA formation (Xu et al.,
85 2015; Lee et al., 2016). Also, the organic nitrates produced in these reactions play an important role in nitrogen
86 chemistry by altering NO_x concentration, which further influences photochemical recycling and ozone
87 formation in the next day. Among these reaction products, HOM can also be formed (Xu et al., 2015; Lee et al.,
88 2016; Yan et al., 2016). Despite the potential importance, studies of HOM formation in the oxidation of BVOC
89 by NO₃ are still limited compared with the HOM formation via oxidation by O₃ and OH. Although a number of
90 laboratory studies have investigated the reaction of NO₃ with BVOC (Ng et al., 2008; Fry et al., 2009; Rollins
91 et al., 2009; Fry et al., 2011; Kwan et al., 2012; Fry et al., 2014; Boyd et al., 2015; Schwantes et al., 2015; Nah
92 et al., 2016; Boyd et al., 2017; Claflin and Ziemann, 2018; Faxon et al., 2018; Draper et al., 2019; Takeuchi and
93 Ng, 2019; Novelli et al., 2021; Vereecken et al., 2021), these studies mostly focus on either SOA yield and
94 composition, or on the gas-phase chemistry mechanism mainly for “traditional” oxidation products that stem
95 from few oxidation steps.

96 Importantly, HOM formation in the reaction of NO₃ with isoprene, the most abundant BVOC accounting
97 for more than half of the global BVOC emissions, has not been explicitly addressed yet, to the best of our
98 knowledge. Although isoprene from plants are mainly emitted under light conditions, i.e., in the daytime,
99 isoprene can remain high after sunset in significant concentrations (Starn et al., 1998; Stroud et al., 2002; Brown et
100 al., 2009) because of the reduced consumption by OH and is found to decay rapidly. A substantial fraction of
101 isoprene can then be oxidized by NO₃ (Brown et al., 2009). Regarding the budget of NO₃, the reaction of isoprene
102 with NO₃ can contribute to a significant or even dominant fraction of NO₃ loss at night in regions where VOC is
103 dominated by isoprene such as Northeast US (Brown et al., 2009). Under some circumstances, the reaction of isoprene
104 with NO₃ can contribute to a significant fraction during the afternoon and afterwards (Ayres et al., 2015; Hamilton
105 et al., 2021). The reaction of isoprene with NO₃ is the subject of a number of studies (Ng et al., 2008; Perring et
106 al., 2009; Rollins et al., 2009; Kwan et al., 2012; Schwantes et al., 2015; Vereecken et al., 2021). These studies
107 focus on the oxidation mechanism and “traditional” oxidation products, as well as SOA yields. The initial step
108 is the NO₃ addition to one of the C=C double bonds, preferentially to the carbon C1 (Schwantes et al., 2015),
109 followed by O₂ addition forming a nitrooxyalkyl peroxy radical (RO₂). This RO₂ can undergo the reactions
110 described above, forming a series of products such as C5-nitrooxyhydroperoxide, C5-nitrooxycarbonyl, and C5-
111 hydroxynitrate (Ng et al., 2008; Kwan et al., 2012), as well as methyl vinyl ketone (MVK), potentially
112 methacrolein (MACR), formaldehyde, OH radical, and NO₂ as minor products (Schwantes et al., 2015). A high

113 nitrate yield (57-95%) was found (Perring et al., 2009; Rollins et al., 2009; Kwan et al., 2012; Schwantes et al.,
114 2015). Products in the particle phase such as C₁₀ dimers were also detected (Ng et al., 2008; Kwan et al., 2012;
115 Schwantes et al., 2015). The SOA yield varies from 2% to 23.8% depending on the organic aerosol concentration
116 (Ng et al., 2008; Rollins et al., 2009). These studies have provided valuable insights in oxidation mechanism,
117 particle yield and composition. However, because HOM formation was not the focus of these studies, only a
118 limited number of products, mainly moderately oxygenated ones (oxygen number ≤ 2 in addition to NO₃
119 functional groups), were detected in the gas phase. The detailed mechanism of HOM formation and their yields
120 in the reaction of BVOC+NO₃ are still unclear.

121 In this study, we investigated the HOM formation in the oxidation of isoprene by NO₃. We report the
122 identification of HOM, including HOM monomers, dimers, and trimers. According to the reaction products and
123 literature, we discuss the formation mechanism of these HOM. The formation mechanism of various HOM is
124 further constrained with time series of HOM upon repeated isoprene additions. We also provide an estimate of
125 HOM yield in the isoprene+NO₃ reaction and assess their roles in SOA formation.

126 **2 Experimental**

127 **2.1 Chamber setup and experiments**

128 Experiments investigating the reaction of isoprene with NO₃ were conducted in the SAPHIR chamber
129 (Simulation of Atmospheric PHotochemistry In a large Reaction chamber) at Forschungszentrum Jülich,
130 Germany. The details of the chamber have been described before (Rohrer et al., 2005; Zhao et al., 2015a; Zhao
131 et al., 2015b; Zhao et al., 2018). Briefly, SAPHIR is a Teflon chamber with a volume of 270 m³. It can utilize
132 natural sunlight for illumination and is equipped with a louvre system to switch between light and dark
133 conditions. In this study, the experiments were conducted in the dark with the louvres closed.

134 Temperature and relative humidity were continuously measured. Gas and particle phase species were
135 characterized using a comprehensive set of instruments with the details described before (Zhao et al., 2015b).
136 VOC were characterized using a Proton Transfer Reaction Time-of-Flight Mass Spectrometer (PTR-ToF-MS,
137 Ionicon Analytik, Austria). NO_x and O₃ concentrations were measured using a chemiluminescence NO_x analyzer
138 (ECO PHYSICS TR480) and an UV photometer O₃ analyzer (ANSYCO, model O341M), respectively. OH,
139 HO₂ and RO₂ concentrations were measured using a laser induced fluorescence system (LIF) (Fuchs et al., 2012).
140 NO₃ and N₂O₅ were detected by a custom-built instrument based on cavity ring-down spectroscopy. The design
141 of the instrument is similar to that described by Wagner et al. (2011). NO₃ was directly detected in one cavity
142 by its absorption at 662 nm and the sum of NO₃ and N₂O₅ in a second, heated cavity, which had a heated inlet
143 to thermally decompose N₂O₅ to NO₃. The sampling flow rate was 3 to 4 liters per minute. The detection by
144 cavity ring-down spectroscopy was achieved by a diode laser that was periodically switched on and off with a
145 repetition rate of 200 Hz. Ring-down events were observed by a digital oscilloscope PC card during the time
146 when the laser was switched off and were averaged over 1s. The zero-decay time that is needed to calculate the
147 concentration of NO₃ was measured every 20 s by chemically removing NO₃ in the reaction with excess nitric

148 oxide (NO) in the inlet system. The accuracy of measurements was limited by the uncertainty in the correction
149 for inlet losses of NO₃ and N₂O₅. In the case of N₂O₅ a transmission of (85±10) % was achieved and in the case
150 of NO₃ of (50±30) %.

151 Before an experiment, the chamber was flushed with high purity synthetic air (purity>99.9999% O₂ and N₂).
152 Experiments were conducted under dry condition (RH<2 %) and temperature was at 302±3 K. NO₂ and O₃ were
153 added to the chamber first to form N₂O₅ and NO₃, reaching concentrations of ~60 ppb for NO₂ and ~100 ppb for O₃.
154 After around half an hour, isoprene was sequentially added into the chamber for three times at intervals of ~1 h.
155 Around 40 min after the third isoprene injection, NO₂ was added to compensate the loss of NO₃ and N₂O₅. Afterwards,
156 three isoprene additions were repeated in the same way as before. O₃ was added before the fifth and the sixth isoprene
157 addition to compensate for its loss by reaction. The schematic for the experimental procedure is shown in Fig. S1.
158 Experiments were designed such that the chemical system was dominated by the reaction of isoprene with NO₃ and
159 the reaction of isoprene with O₃ did not play a major role (<3% of the isoprene consumption). Figure S2 shows the
160 relative contributions of the reaction of O₃ and NO₃ with isoprene to the total chemical loss of isoprene using the
161 NO₃ and O₃ concentrations measured. The reaction with NO₃ accounted for >95% of the isoprene consumption for
162 the whole experiments. The contribution of the reaction of isoprene with trace amount of OH, mainly produced in
163 the reaction of isoprene+O₃ via Criegee intermediates (Nguyen et al., 2016), is negligible as the OH yield is less than
164 one (Malkin et al., 2010) and thus its contribution is less than that of isoprene+O₃. This is consistent with the
165 contribution determined using measured OH concentration, despite some uncertainty in measured OH concentration
166 due to the interference from NO₃. In these experiments, RO₂ fate is estimated to be dominated by its reaction with
167 NO₃ according to the measured NO₃, RO₂, and HO₂ concentration and their rate constants for the reactions with RO₂
168 (MCM v3.2(Jenkin et al., 1997; Jenkin et al., 2003; Saunders et al., 2003; Jenkin et al., 2015), via website:
169 <http://mcm.leeds.ac.uk/MCM>) despite uncertainties of the measured RO₂ and HO₂ concentration due to interference
170 from NO₃. As a large portion of RO₂ is not measured by LIF (Vereecken et al., 2021) and thus RO₂ is underestimated,
171 we expected the reaction of RO₂+RO₂ to be also important. Overall, we estimate that the RO₂ fate is dominated the
172 reaction RO₂+NO₃ with significant contribution of RO₂+RO₂.

173 2.2 Characterization of HOM

174 In this study we refer to similar definition for HOM by Bianchi et al. (2019), i.e., HOM typically contain six or
175 more oxygen atoms formed via autoxidation and related chemistry of peroxy radicals. HOM were detected using a
176 Chemical Ionization time-of-flight Mass Spectrometer (Aerodyne Research Inc., USA) with nitrate as the reagent ion
177 (CIMS) (Eisele and Tanner, 1993; Jokinen et al., 2012). ¹⁵N nitric acid was used to produce ¹⁵NO₃⁻ in order to
178 distinguish the NO₃ group in target molecules formed in the reaction from the reagent ion. The details of the
179 instrument are described in our previous publications (Ehn et al., 2014; Mentel et al., 2015; Pullinen et al., 2020).
180 The CIMS has a mass resolution of ~4000 (m/dm). Examples of peak fitting are shown in Fig. S3. HOM
181 concentrations were estimated using the calibration coefficient of H₂SO₄ as described by Pullinen et al. (2020)
182 because the charge efficiency of HOM and H₂SO₄ can be assumed to be equal and close to the collision limit (Ehn et
183 al., 2014; Pullinen et al., 2020). The details of the calibration with H₂SO₄ are provided in the supplement S1. Since
184 HOM contain more than six oxygen atoms and their clusters with nitrate ions are quite stable (Ehn et al., 2014), the

185 charge efficiency of HOM is thus assumed to be equal to that of H₂SO₄, which is close to the collision limit (Viggiano
186 et al., 1997). If HOM do not charge with nitrate ions at their collision limit or the clusters formed break during the
187 short residence time in the charger, its concentration would be underestimated as pointed by Ehn et al. (2014). Thus,
188 our assumption provides a lower limit of the HOM concentration. The HOM yield was derived using the
189 concentration of the HOM produced, divided by the concentration of isoprene that was consumed by NO₃. The
190 uncertainty of HOM yield was estimated to -55%/+103%. The loss of HOM to the chamber was corrected using a
191 wall loss rate of 6×10⁻⁴ s⁻¹ as quantified previously (Zhao et al., 2018). HOM concentrations were also corrected for
192 dilution due to the replenishment flow needed to maintain a constant overpressure of the chamber (loss rate ~1×10⁻⁶
193 s⁻¹) (Zhao et al., 2015b). The influence of wall loss correction and dilution correction on HOM yield was ~12% and
194 <1%, respectively. Although the wall loss rate of vapors in this study might not be exactly the same as in our previous
195 photo-oxidation experiments (Zhao et al., 2018), HOM yield is not sensitive to the vapor wall loss rate. An increase
196 of wall loss rate by 100% or a decrease by 50% only changes the HOM yield by 11% and -6%, respectively.

197 **3 Results and discussion**

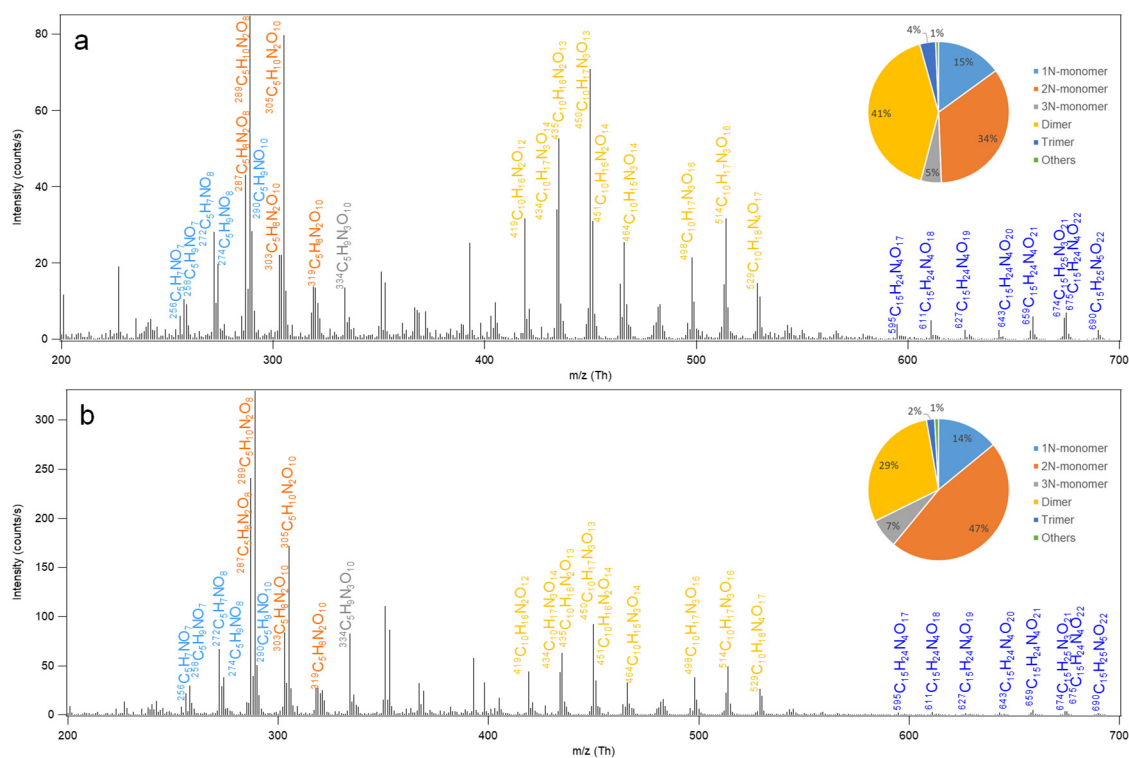
198 **3.1 Overview of HOM**

199 The mass spectra of HOM in the gas phase formed in the oxidation of isoprene by NO₃ are shown in
200 Fig. 1. A large number of HOM were detected. Almost all peaks are assigned HOM containing nitrogen atoms
201 with possibly few exceptions such as C₅H₁₀O₈ and C₅H₈O₁₁ with very minor peaks (<~1% of the maximum
202 peak). The reaction products can be roughly divided into three classes: monomers (C₅, ~200-400 Th), dimers
203 (C₁₀, ~400-600 Th), and trimers (C₁₅, ~>600 Th), according to their mass to charge ratio (m/z). The detailed
204 peak assignment of monomers, dimers, and trimers is discussed in the following sections.

205 **3.2 HOM monomers and their formation**

206 **3.2.1 Overview of HOM monomers**

207 HOM monomers showed a roughly repeating pattern in the mass spectrum at every 16 Th
208 (corresponding to the mass of oxygen) (Fig. 1a). Here a number of series of HOM monomers with continuously
209 increasing oxygenation were found, such as C₅H₉NO_n, C₅H₇NO_n, C₅H₈N₂O_n, C₅H₁₀N₂O_n (Table 1, Table S1-2
210 and Fig. 2). These monomers included both stable closed-shell molecules and open-shell radicals, such as
211 C₅H₈NO_n• and C₅H₉N₂O_n•. The open-shell molecules were likely RO₂ radicals because of their much longer life
212 time and hence higher concentrations compared with alkoxy radicals (RO) and alkyl radicals (R). Since the
213 observed stable products were mostly termination products of RO₂ reactions, we describe the stable products in
214 a RO₂-oriented approach. It is worth noting that some of the termination products may contain multiple isomers
215 formed from different pathways.

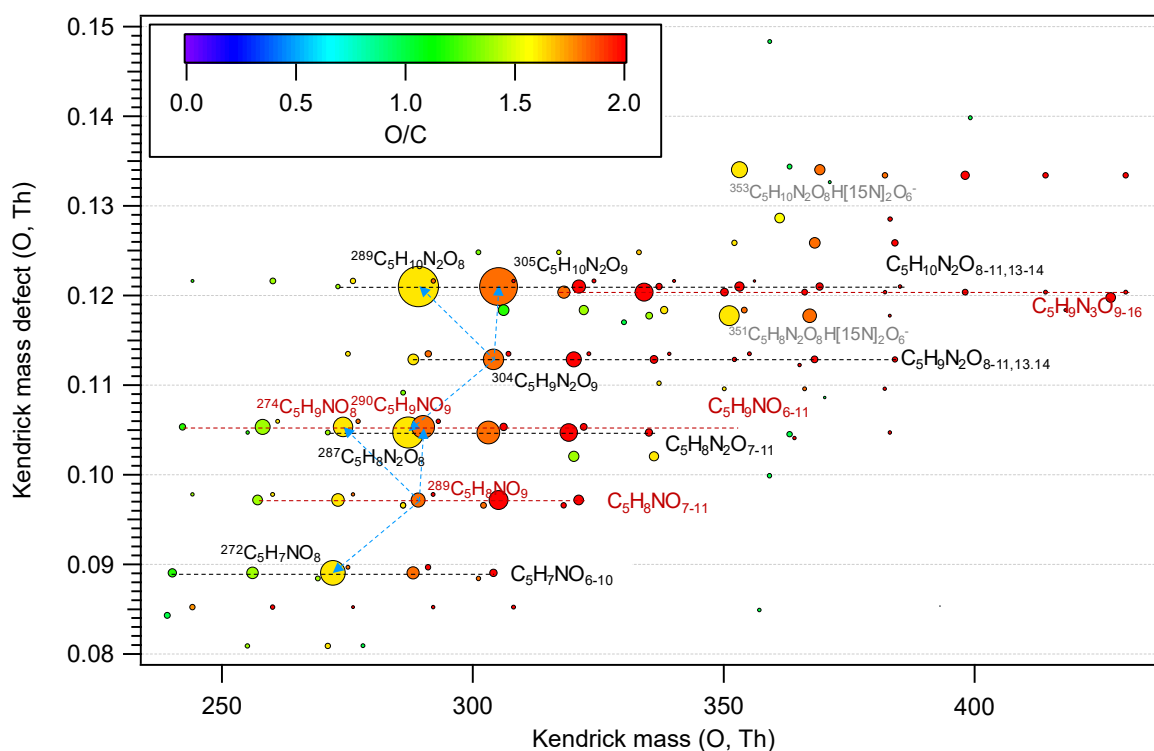


216

217

218 Figure 1. Mass spectrum of the HOM formed in the oxidation of isoprene by NO_3 . HOM are detected as
 219 clusters with the reagent ion $^{15}\text{NO}_3^-$, which is not shown in the molecular formula in the figure for simplicity. Panel
 220 a and b show the average spectrum during the first isoprene addition period (P1) and for the whole period of six
 221 isoprene additions (P1-6), respectively. The insets show the contributions of different classes of HOM. 1-3N-
 222 monomer refers to the monomers containing 1-3 nitrogen atoms in the molecular formula.

223 HOM monomers were classified into 1N-, 2N-, and 3N-monomers according to the number of nitrogen
 224 atoms that they contain. HOM without nitrogen atoms were barely observed except for very minor peaks ($< \sim 1\%$
 225 of the maximum peak) possibly assigned to $\text{C}_5\text{H}_{10}\text{O}_8$ and $\text{C}_5\text{H}_8\text{O}_{11}$. The contribution of 2N-monomers such as
 226 $\text{C}_5\text{H}_{10}\text{N}_2\text{O}_n$ and $\text{C}_5\text{H}_8\text{N}_2\text{O}_n$ was higher than that of the 1N-HOM monomers, and that of 3N-monomers was the least
 227 (Fig. 1, inset). The most abundant monomers were $\text{C}_5\text{H}_{10}\text{N}_2\text{O}_8$, $\text{C}_5\text{H}_{10}\text{N}_2\text{O}_9$, and $\text{C}_5\text{H}_8\text{N}_2\text{O}_8$. The termination products
 228 of $\text{C}_5\text{H}_9\text{NO}_8$, $\text{C}_5\text{H}_9\text{NO}_9$, and $\text{C}_5\text{H}_7\text{NO}_8$ also showed relatively high abundance. These limited number of compounds
 229 dominated the HOM monomers. Since 2N-monomers were second-generation products as discussed below, the
 230 higher abundance 2N- monomers indicate that the second-generation HOM play an important role in the reaction of
 231 NO_3 with isoprene in the reaction conditions of our study, as also seen by Wu et al. (2020). This is more evident for
 232 the mass spectrum averaged over six isoprene addition periods (Fig. 1b), where the abundance of $\text{C}_5\text{H}_{10}\text{N}_2\text{O}_n$ and
 233 $\text{C}_5\text{H}_8\text{N}_2\text{O}_n$ were more dominant. This observation is in contrast with the finding for the reaction of O_3 with BVOC
 234 which contains only one double bond such as α -pinene (Ehn et al., 2014), where HOM are mainly first-generation
 235 products formed via autoxidation. The higher abundance of HOM 2N-monomers than 1N-monomers is likely because
 236 HOM production rate via the autoxidation of 1N-monomer RO_2 following the reaction of isoprene with NO_3 may be
 237 slower than that of the reaction of 1N-monomers (including both HOM and non-HOM monomers) with NO_3 . We
 238 would like to note that some less oxygenated 1N-monomers such as $\text{C}_5\text{H}_9\text{NO}_{4/5}$ and $\text{C}_5\text{H}_7\text{NO}_4$ may have high
 abundance but are not detected by NO_3^- -CIMS and are not HOM and thus not included in HOM 1N-monomers.



239

240

241

242

243

244

245

Figure 2. Kendrick mass defect plot for O of HOM monomers. The m/z in the molecular formula include the reagent ion $^{15}\text{NO}_3^-$, which is not shown for simplicity. The size (area) of circles is set to be proportional to the average peak intensity of each molecular formula during the first isoprene addition period (P1). The species at m/z 351 and 353 (labelled in grey) are the adducts of $\text{C}_5\text{H}_8\text{N}_2\text{O}_8$ and $\text{C}_5\text{H}_{10}\text{N}_2\text{O}_8$ with $\text{H}[^{15}\text{N}]_2\text{O}_6^-$, respectively. The blue dashed lines with arrows indicate the termination product hydroperoxide (M+H), alcohol (M-O+H), and ketone (M-O-H) with M the molecular formula of a HOM RO_2 .

246

3.2.2 1N-monomers

247

248

249

250

251

252

In our experiments we observed a $\text{C}_5\text{H}_8\text{NO}_n\cdot$ ($n=7-12$) series (series M1), as well as its corresponding termination products $\text{C}_5\text{H}_7\text{NO}_{n-1}$, $\text{C}_5\text{H}_9\text{NO}_{n-1}$, and $\text{C}_5\text{H}_9\text{NO}_n$ via the reactions with RO_2 and HO_2 , which contain carbonyl, hydroxyl, and hydroperoxy group, respectively. Overall, the peak intensities of $\text{C}_5\text{H}_9\text{NO}_n$ and $\text{C}_5\text{H}_7\text{NO}_n$ series first increased and then decreased as oxygen number increased (Fig. 2), with the peak intensity of $\text{C}_5\text{H}_9\text{NO}_8$ and $\text{C}_5\text{H}_7\text{NO}_8$ being the highest within their respective series when averaged over the whole experiment period.

253

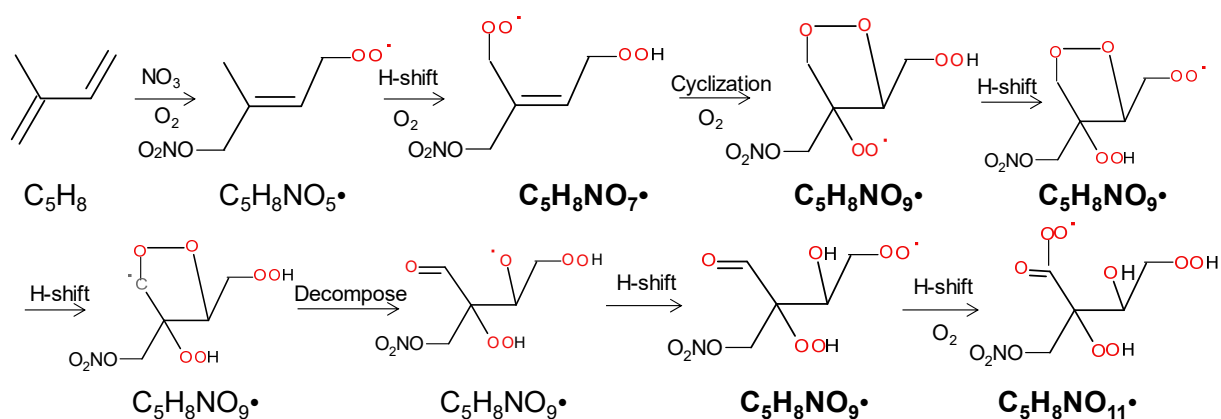
Table 1. HOM monomers formed in the oxidation of isoprene by NO_3 .

Series Number	Product	Type ^a	Pathway of RO_2
M1a/b	$\text{C}_5\text{H}_8\text{NO}_n$ ($n=7-11$)	RO_2	Isoprene+ NO_3
	$\text{C}_5\text{H}_9\text{NO}_n$ ($n=6-11$)	ROOH/ROH	Isoprene+ NO_3 + NO_3
	$\text{C}_5\text{H}_7\text{NO}_n$ ($n=6-10$)	R=O	
M2a/b	$\text{C}_5\text{H}_9\text{N}_2\text{O}_n$ ($n=8-11,13,14$) ^b	RO_2	
	$\text{C}_5\text{H}_{10}\text{N}_2\text{O}_n$ ($n=8-11,13,14$) ^b	ROOH/ROH	Isoprene + NO_3 + NO_3
	$\text{C}_5\text{H}_8\text{N}_2\text{O}_n$ ($n=7-11$)	R=O	

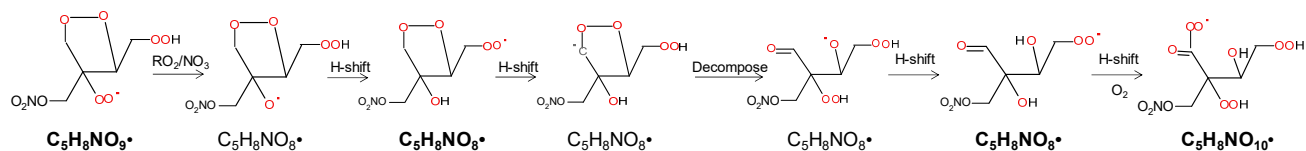
	$C_5H_9N_3O_n$ (n=9-16) ^b	RO_2NO_2	
M3	$C_5H_7N_2O_n$ (n=9)	RO_2	
	$C_5H_8N_2O_n$ (n=8, 9)	ROOH/ROH	Isoprene +NO ₃ +NO ₃
	$C_5H_6N_2O_n$ (n=8)	R=O	
M4	$C_5H_{10}NO_n$ (n=8-9)	RO_2	
	$C_5H_{11}NO_n$ (n=7-9)	ROOH/ROH	Isoprene +NO ₃ +OH
	$C_5H_9NO_n$ (n=7-8)	R=O	

254 ^a: RO₂ denotes peroxy radical and ROOH, ROH, R=O, and RO₂NO₂ denote the termination products
 255 containing hydroperoxy, hydroxyl, carbonyl group, and peroxyxynitrate, respectively.

256 ^b: Peak assignment of compounds with n=13,14 may be subject to uncertainties.



(a)



(b)

262 Scheme 1. The example pathways to form HOM RO₂ C₅H₈NO_n• (n=7, 9, 11) series (a) and C₅H₈NO_n•
 263 (n=8, 10) series (b) in the reaction of isoprene with NO₃. The detected products are in bold.

264 C₅H₈NO_n• with odd number oxygen atoms (n=7, 9, 11, series M1a) were possibly formed by the attack
 265 of NO₃ to one double bond (preferentially to C1 according to previous studies (Skov et al., 1992; Berndt and
 266 Böge, 1997; Schwantes et al., 2015) and followed by autoxidation (Scheme 1a). We would like to note that
 267 NO₃⁻-CIMS only observed HOM with oxygen numbers ≥ 6 in this study due to its selectivity of detection.
 268 C₅H₈NO_n• with even number oxygen atoms (n=8, 10, series M1b in Table 1) were possibly formed after H-shift
 269 of an alkoxy radical formed in reaction R4 or R5 and subsequent O₂ addition (“alkoxy-peroxy” channel)
 270 (Scheme 1b), where the alkoxy radicals can be formed both from the RO₂+NO₃ and RO₂+RO₂ reactions. The
 271 hydroxyRO₂ formed can undergo further autoxidation adding two oxygen atoms after each H-shift. We would
 272 like to note that the scheme and other schemes in this study only show example isomers and pathways to form these

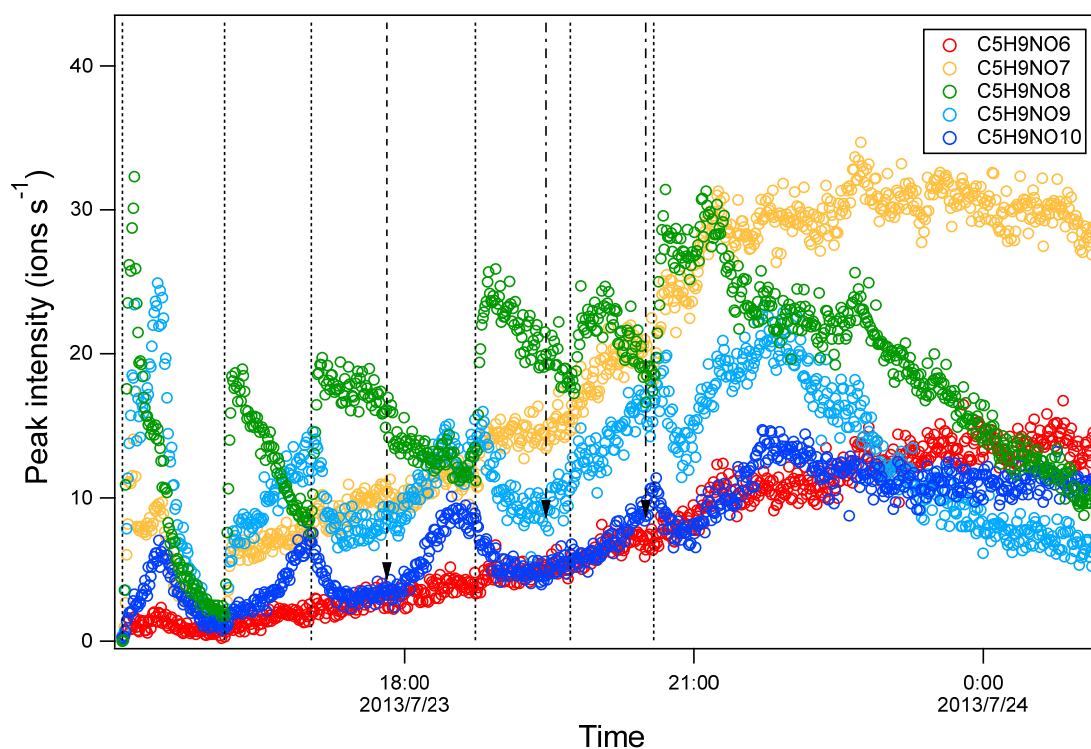
273 molecules. It is likely that many of the reactions occurring are not the dominant channels as otherwise there would
274 be much higher HOM yield as discussed below.

275 Some HOM monomers may contain multiple isomers and be formed via different pathways. For
276 example, $C_5H_9NO_n$ can contain alcohols derived from $RO_2 C_5H_8NO_{n+1}\bullet$, hydroperoxides derived from RO_2
277 $C_5H_8NO_n\bullet$ or the ketones from $RO_2 C_5H_{10}NO_{n+1}\bullet$. Some $RO_2 C_5H_8NO_n\bullet$ may be formed via the reaction of first-
278 generation products with NO_3 in addition to direct reaction of isoprene with NO_3 . For example, $C_5H_8NO_7\bullet$ can
279 be formed by the reaction of NO_3 with $C_5H_8O_2$, which is a first-generation product observed previously in the
280 reaction of isoprene with NO_3 or OH (Scheme S1b) (Kwan et al., 2012). Moreover, $RO_2 C_5H_8NO_n\bullet$ can be
281 formed from C5-carbonylnitrate, a first-generation product, with OH (Scheme S1a). Trace amount of OH can
282 be produced in the reaction of isoprene with NO_3 (Kwan et al., 2012; Wennberg et al., 2018). OH can also be
283 formed via Criegee intermediates formed in the isoprene+ O_3 reaction (Nguyen et al., 2016), but this OH source
284 was likely minor because the contribution of the isoprene+ O_3 reaction to total isoprene loss was negligible (<5%,
285 Fig. S2). In addition, $C_5H_8NO_8\bullet$ may also be formed by the reaction of NO_3 with $C_5H_8O_3$, which is a first-
286 generation product observed in the reaction of isoprene with OH (Kwan et al., 2012). The $C_5H_8NO_n\bullet$ formed
287 via direct reaction of isoprene with NO_3 is a first-generation RO_2 while that formed via other indirect pathways
288 is a second-generation RO_2 . The time profile of the isomers from these two pathways, however, are expected to
289 be different as will be discussed below.

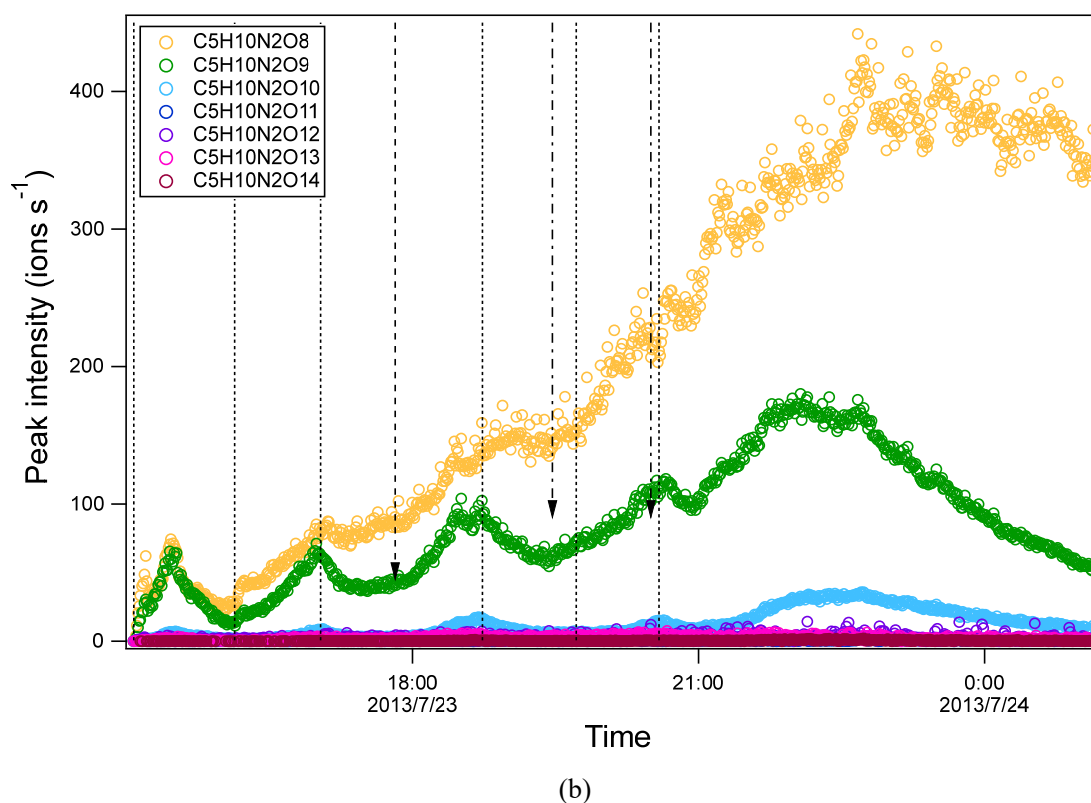
290 Time series of HOM can shed light on their formation mechanisms. It is expected that first-generation
291 products increase fast with isoprene addition and reach a maximum earlier in the presence of wall loss of organic
292 vapour, while second-generation products reach a maximum in the later stage or increase continuously if the
293 production rate is higher than the loss rate. As a reference to analyze the time profiles of HOM, the times profile
294 of isoprene, NO_3 , and N_2O_5 are also shown (Fig. S4). After isoprene was added in each period, NO_3 and N_2O_5
295 dropped dramatically and then gradually increased. We found that termination products within the same M1
296 series showed different time profiles. For example, in $C_5H_9NO_n$ series, $C_5H_9NO_8$ clearly increased
297 instantaneously with isoprene addition, and decreased fast afterwards (Fig. 3a), indicating that it was a first-
298 generation product, which was expected according to the mechanism Scheme 1. $C_5H_9NO_6$ and $C_5H_9NO_{10}$ had a
299 general increasing trend with time. While $C_5H_9NO_6$ increased continuously with time, $C_5H_9NO_{10}$ reached
300 maximum intensity in the late phase of each isoprene addition period and then decreased naturally or after
301 isoprene addition. The faster loss of $C_5H_9NO_{10}$ than $C_5H_9NO_6$ may result from the faster wall loss due to its
302 lower volatility. $C_5H_9NO_7$ and $C_5H_9NO_9$ showed a mixing time profile with features of the former two kinds of
303 time profiles, increasing almost instantaneously with isoprene additions, especially in the first two periods,
304 while increasing continuously or decreasing first with isoprene additions and then increasing later in each period.
305 This kind of time series indicates that there were significant contributions from both first- and second-generation
306 products.

307 The second-generation products may be different isomers formed in pathways other than shown in
308 Scheme 1. Second-generation $C_5H_9NO_6$ can be formed via $C_5H_8NO_7\bullet$, which can also be formed by the reaction
309 of NO_3 and O_2 with $C_5H_8O_2$ as mentioned above (Scheme S2b), or by the reaction of OH with $C_5H_7NO_4$ (Scheme

310 S2a). The time profiles of $C_5H_8NO_7\bullet$ did show more contribution of second-generation processes because it
311 continuously increased with time in general. If the pathways via the reaction of NO_3 and O_2 with $C_5H_8O_2$ and
312 the reaction of OH with $C_5H_7NO_4$ contribute most to $C_5H_9NO_6$, $C_5H_9NO_6$ would show mostly a time profile of
313 second-generation products. Similarly, second-generation $C_5H_9NO_7$ can be formed via $C_5H_8NO_7\bullet$ or $C_5H_8NO_8\bullet$.
314 The time series of $C_5H_8NO_8\bullet$ did show the contribution of both the first- and second-generation processes, which
315 generally increased with time while also responding to isoprene addition (Fig. S5). Similar to $C_5H_9NO_6$, the
316 second-generation pathway for $C_5H_9NO_7$, $C_5H_9NO_9$, and $C_5H_9NO_{10}$ are shown in Scheme S1, S3, S4. For the
317 RO_2 in $C_5H_8NO_n\bullet$ series other than $C_5H_8NO_{7/8}\bullet$, the peak of $C_5H_8NO_n\bullet$ overlaps with $C_5H_{10}N_2O_n$ in the mass
318 spectra, which is a much larger peak, and thus cannot be differentiated from $C_5H_{10}N_2O_n$. Therefore, it is not
319 possible to obtain reliable separate time profiles in order to differentiate their major sources. It is worth noting
320 that nitrate CIMS may not be able to detect all isomers of $C_5H_9NO_6$ due to the sensitivity limitation. Therefore,
321 we cannot exclude the possibility that the absence of some first-generation isomers of $C_5H_9NO_6$ was due to the
322 low sensitivity of these isomers.



(a)



325
326

327 Figure 3. Time series of peak intensity of several HOM monomers of $C_5H_9NO_n$ series (a) and of $C_5H_{10}N_2O_n$
328 series (b). They are likely the termination products of RO_2 $C_5H_8NO_n^\bullet$ and $C_5H_9N_2O_n^\bullet$, respectively. The dashed lines
329 indicate the time of isoprene additions. The long-dashed arrow indicates the time of NO_2 addition. The dash-dotted
330 arrows indicate the time of O_3 additions.

331 Among the termination products of the 1N-monomer RO_2 , carbonyl and hydroxyl/hydroperoxide
332 species had comparable abundance in general (Table S1), suggesting that disproportionation reactions between
333 RO_2 and RO_2 forming hydroxy and carbonyl species (R1-2) was likely an important RO_2 termination pathway.
334 However, dependence of the exact ratio of carbonyl species to hydroxyl/hydroperoxide species on the number
335 of oxygen atoms did not show a clear trend (Table S1), suggesting that the reactions of HOM RO_2 depended on
336 their specific structure. There was no clear difference in the abundance between the termination products from
337 $C_5H_8NO_n^\bullet$ with odd and even number of oxygen atom in general, although the most abundant termination
338 product of $C_5H_8NO_n^\bullet$, i.e. $C_5H_7NO_8$, was likely formed from $C_5H_8NO_9^\bullet$ in series M1a. This fact indicates that
339 both the peroxy pathway and alkoxy-peroxy pathway were important for the HOM formation in the
340 isoprene+ NO_3 reaction under our conditions, in agreement with the significant formation of alkoxy radicals
341 from the reaction of RO_2 with NO_3 and RO_2 .

342 In addition to the termination products of RO_2 M1, minor peaks of the RO_2 series $C_5H_{10}NO_n^\bullet$ ($n=8-9$) (M4,
343 Table 1) and their corresponding termination products including hydroperoxide, alcohol and carbonyl species were
344 detected (Table S3). $C_5H_{10}NO_n$ were likely formed by sequential addition of NO_3 and OH to two double bonds of
345 isoprene (Scheme S5). OH can react fast with isoprene or with the first-generation products of the reaction of isoprene

346 with NO_3 , thus forming $\text{C}_5\text{H}_{10}\text{NO}_n^\bullet$. In addition, a few very minor but noticeable peaks of $\text{C}_5\text{H}_9\text{O}_n^\bullet$ and their
347 corresponding termination products $\text{C}_5\text{H}_{10}\text{O}_n$ and $\text{C}_5\text{H}_8\text{O}_n$ were also observed. These HOM may be formed by the
348 reactions of isoprene with trace amount of OH and with O_3 , although their contributions to reacted isoprene were
349 negligible. These HOM were also observed in the reaction of isoprene with O_3 with and without OH scavengers
350 (Jokinen et al., 2015).

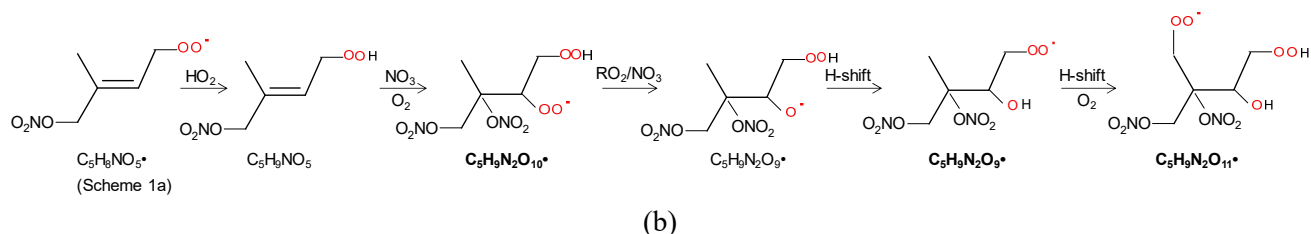
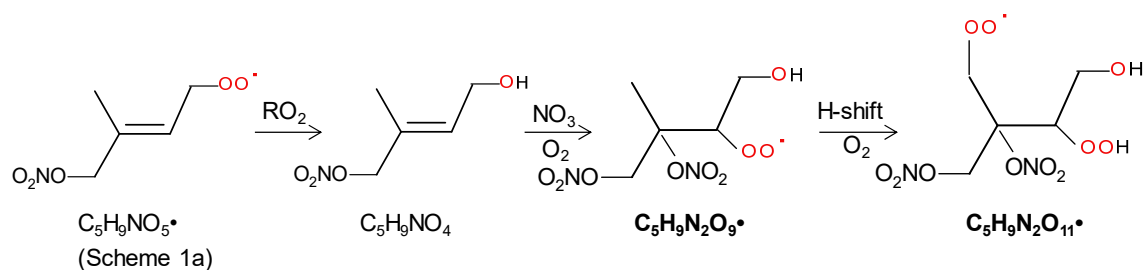
351 Among 1N-monomer HOM, $\text{C}_5\text{H}_9\text{NO}_7$ has been observed in the particle phase using ESI-TOFMS by
352 Ng et al. (2008) while others have not been observed in previous laboratory studies of the reaction of isoprene
353 with NO_3 , to our knowledge. A number of C_5 organic nitrates have been observed in field studies. For example,
354 $\text{C}_5\text{H}_{7-11}\text{NO}_{6-8}$ and $\text{C}_5\text{H}_{7-11}\text{NO}_{4-9}$ have been observed in the gas phase (Massoli et al., 2018) and the particle phase
355 (Lee et al., 2016; Chen et al., 2020), respectively in a rural area of southeast US, where isoprene is abundant.
356 Xu et al. (2021) observed a number of C_5 1N-HOM such as $\text{C}_5\text{H}_{7,9,11}\text{NO}_{6,7}$ in polluted megacities of Nanjing
357 and Shanghai of east China during summer. While many of these HOM have daytime sources and are attributed
358 to photo-oxidation in the presence of NO_x , nighttime oxidation with NO_3 also contribute to their formation (Lee
359 et al., 2016; Chen et al., 2020; Xu et al., 2021). $\text{C}_5\text{H}_{7-11}\text{NO}_{4-9}$ were also observed in chamber experiments of the
360 reaction of isoprene with OH in the presence of NO_x (Lee et al., 2016). $\text{C}_5\text{H}_x\text{NO}_{4-9}$ and $\text{C}_5\text{H}_x\text{NO}_{4-10}$ have been
361 also observed in the gas phase and particle phase, respectively, in a monoterpene-dominating rural area in
362 southwest Germany (Huang et al., 2019).

363 3.2.3 2N-monomers

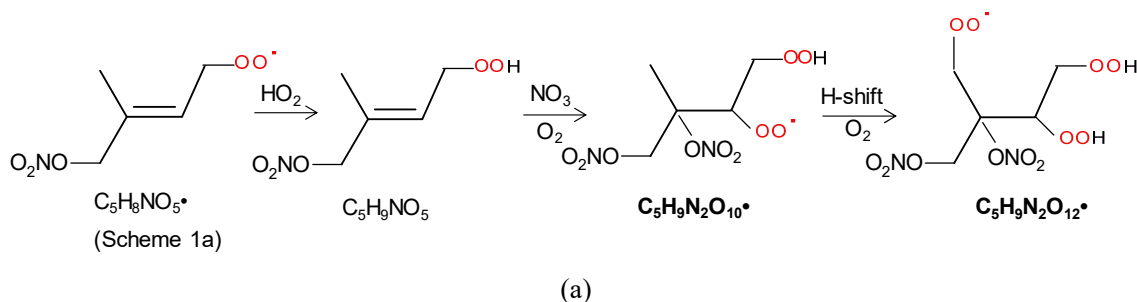
364 The 2N-monomer RO_2 series $\text{C}_5\text{H}_9\text{N}_2\text{O}_n^\bullet$ ($n=8-14$), were observed, as well as its likely termination
365 products, $\text{C}_5\text{H}_8\text{N}_2\text{O}_n$ and $\text{C}_5\text{H}_{10}\text{N}_2\text{O}_n$, which contain a carbonyl and hydroxyl or hydroperoxide functional group,
366 respectively. The RO_2 series $\text{C}_5\text{H}_9\text{N}_2\text{O}_n^\bullet$ with odd number of oxygen atoms ($n=9, 11$) (M2a in Table 1) were
367 likely formed from the first-generation product $\text{C}_5\text{H}_9\text{NO}_4$ (C_5 -hydroxynitrate) by adding NO_3 to the remaining
368 double bond, forming $\text{C}_5\text{H}_9\text{N}_2\text{O}_9^\bullet$, followed by autoxidation (Scheme 2a). This RO_2 series can also be formed
369 by the addition of NO_3 to the double bond of first-generation products (e.g. $\text{C}_5\text{H}_9\text{NO}_5$, C_5 -
370 nitrooxyhydroperoxide) and a subsequent alkoxy-peroxy step (Scheme 2b). $\text{C}_5\text{H}_9\text{N}_2\text{O}_n^\bullet$ with even number of
371 oxygen atoms ($n=8, 10, 12$) (M2b in Table 1), can be formed by the addition of NO_3 to the double bond of
372 $\text{C}_5\text{H}_9\text{NO}_5$ followed by autoxidation (Scheme. 3a), or of $\text{C}_5\text{H}_9\text{NO}_4$ followed by an alkoxy-peroxy step (Scheme.
373 3b). The formation pathways of $\text{C}_5\text{H}_9\text{N}_2\text{O}_{13/14}^\bullet$ and $\text{C}_5\text{H}_9\text{N}_2\text{O}_8^\bullet$ cannot be well explained, as they contain too
374 many or too few oxygen atoms to be formed via the pathways in Scheme 2 or 3. In Scheme 2 and 3, we show the
375 reactions starting from 1- NO_3 -isoprene-4-OO as an example. In the supplement, we have also shown the pathways
376 starting from 1- NO_3 -isoprene-2-OO peroxy radicals, which is indicated in a recent study by Vereecken et al. (2021)
377 to be the dominant RO_2 in the reaction of isoprene with NO_3 .

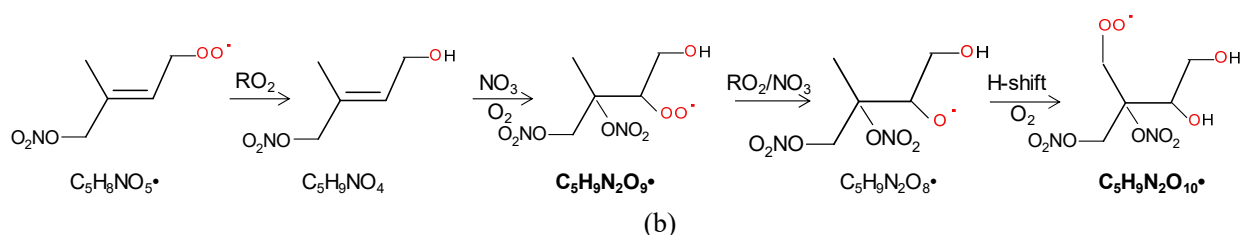
378 Formation through either Scheme 2 or 3 means that $\text{C}_5\text{H}_8\text{N}_2\text{O}_n$ and $\text{C}_5\text{H}_{10}\text{N}_2\text{O}_n$ were second-generation
379 products. The time series of $\text{C}_5\text{H}_{10}\text{N}_2\text{O}_n$ species clearly indicates that they were indeed second-generation
380 products. $\text{C}_5\text{H}_{10}\text{N}_2\text{O}_n$ species generally did not increase immediately with isoprene addition (Fig. 3b), but
381 increased gradually with time and reached its maximum in the later stage of each period before decreasing with

382 time (in the period 1 and 6), or decreasing after the next isoprene addition (periods 2-5). This time profile can
 383 be explained by the time series of the precursor of $C_5H_{10}N_2O_n$, $C_5H_9N_2O_n \cdot (RO_2)$ (Fig. S6). The changing rate
 384 (production rate minus destruction rate) of $C_5H_{10}N_2O_n$ concentration was dictated by the concentration of
 385 $C_5H_9N_2O_n \cdot$ and the wall loss rate. During periods 2 to 5, $C_5H_9N_2O_n \cdot$ gradually increased but decreased sharply
 386 after the isoprene additions, resulted from chemical reactions of $C_5H_9N_2O_n \cdot$ and additionally from wall loss.
 387 When the rate of change of the $C_5H_{10}N_2O_n$ concentration was positive, the concentration of $C_5H_{10}N_2O_n$ increased
 388 with time. After isoprene additions, the rate of change of the $C_5H_{10}N_2O_n$ concentration decreased dramatically
 389 to even negative, leading to decreasing concentrations. Similar to $C_5H_{10}N_2O_n$, the $C_5H_8N_2O_n$ series did not
 390 respond immediately to isoprene additions (Fig. S7), which is expected for second-generation products
 391 according to the mechanism discussed above (Scheme 2-3). Particularly, the continuing increase of $C_5H_8N_2O_n$
 392 even after isoprene was completely depleted (at ~21:40, Fig. S7) clearly indicates that these compounds were
 393 second-generation products, although in the end they decreased due to wall loss.



399 Scheme 2. The example pathways to form $C_5H_9N_2O_n$ ($n=9, 11$) HOM RO_2 series by RO_2 channel (a)
 and alkoxy-peroxy channel. The detected products are in bold.





403
404
405
406

Scheme 3. The example pathways to form $C_5H_9N_2O_n$ ($n=10, 12$) HOM RO_2 series by RO_2 channel (a) and alkoxy-peroxy channel (b). The detected products are in bold.

407
408
409
410
411
412

According to the finding of Ng et al. (2008), C5-hydroxynitrate decays much faster than C5-nitrooxyhydroperoxides. Additionally, C5-hydroxynitrate concentration is expected to be higher than that of nitrooxyhydroperoxides because RO_2+RO_2 forming alcohol is likely more important than RO_2+HO_2 forming hydroperoxide in this study. Therefore, it is likely that $C_5H_9N_2O_n$ M2a series was mainly formed from $C_5H_9NO_4$ instead of $C_5H_9NO_5$, while $C_5H_9N_2O_n$ M2b were formed from $C_5H_9NO_4$ followed by an alkoxy-peroxy step. That is, Scheme 2a and 3b appear more likely.

413
414
415
416
417
418
419
420

Similar to $C_5H_8NO_n$, the intensity of carbonyl species from $C_5H_9N_2O_n$ was also comparable with that of hydroxyl/hydroperoxide species, suggesting that RO_2+RO_2 reaction forming ketone and alcohol was likely an important pathway of HOM formation in the isoprene+ NO_3 reaction. In general, the intensity of the termination products from $C_5H_9N_2O_n$ with both even and odd oxygen numbers were comparable. This again suggests that both peroxy and alkoxy-peroxy pathways were important for HOM formation in the isoprene+ NO_3 reaction. The intensity of $C_5H_8N_2O_n$ first increased and then decreased with oxygen number while $C_5H_{10}N_2O_n$ decreased with oxygen number, with $C_5H_{10}N_2O_8$ and $C_5H_8N_2O_8$ being the most abundant within their respective series.

421
422
423
424
425
426
427
428
429
430
431

Some 2N-monomers have been detected in previous studies of the reaction of isoprene with NO_3 . $C_5H_{10}N_2O_8$ has been detected in the particle phase by Ng et al. (2008) and $C_5H_8N_2O_7$ was detected in the gas phase by Kwan et al. (2012). $C_5H_9N_2O_9$ has been proposed to be formed via the pathway as in Scheme 2a (Ng et al., 2008), and it was directly detected in our study. $C_5H_8N_2O_7$ species has been proposed to be a dinitrooxy epoxide formed by the oxidation of nitrooxyhydroperoxide (Kwan et al., 2012), instead of being a dinitrooxy ketone proposed in our study, a termination product of $C_5H_9N_2O_8$. Admittedly, $C_5H_8N_2O_7$ may contain both isomers. In addition, Ng et al. (2008) detected $C_5H_8N_2O_6$ in the gas phase, which was not detected in this study likely due to the selectivity of NO_3^- -CIMS. 2N-monomers have also been observed in previous field studies. For example, Massoli et al. (2018) observed $C_5H_{10}N_2O_{8-10}$ in rural Alabama US during the SOAS campaign. Xu et al. (2021) observed $C_5H_{8,10}N_2O_8$ and $C_5H_{10}N_2O_8$ in polluted megacities of Nanjing and Shanghai during summer.

432
433
434
435

One could suppose that $C_5H_7N_2O_n$ should also be formed since C5-nitrooxycarbonyl ($C_5H_7NO_4$) also contains one double bond that can be attacked by NO_3 in a second oxidation step. However, concentrations of $C_5H_7N_2O_n$ were too low to assign molecular formulas with confidence except for $C_5H_7N_2O_9$, clearly showing that $C_5H_7N_2O_n$ was not important. This fact is consistent with the finding of Ng et al. (2008) that C5-

436 nitrooxycarbonyls react slowly with NO₃. Additionally, the peroxy radical formed in the reaction of C5-
437 nitrooxycarbonyls with NO₃ likely leads to more fragmentation in H-shift as found in the OH oxidation of
438 methacrolein (Crounse et al., 2012), which may also contribute to the low abundance of C₅H₇N₂O_n. The presence of
439 HOM containing two N atoms is in line with the finding by Faxon et al. (2018) who detected products containing
440 two N atoms in the reaction of NO₃ with limonene, which also contain two carbon double bonds. It is anticipated
441 that for VOC with more than one double bond, NO₃ can add to all the double bonds as for isoprene and limonene.

442 3.2.4 3N-monomers

443 HOM containing three nitrogen atoms, C₅H₉N₃O_n (n=9-16), were observed. These compounds were
444 possibly peroxy nitrates formed by the reaction of RO₂ (C₅H₉N₂O_n•) with NO₂. The time series of C₅H₉N₃O_n
445 was examined to check whether they match such a mechanism. If C₅H₉N₃O_n were formed by the reaction of
446 C₅H₉N₂O_{n-2}• with NO₂, the concentration would be a function of the concentrations of C₅H₉N₂O_{n-2}• and NO₂ as
447 follows:

$$448 \frac{d[C_5H_9N_3O_n]}{dt} = k[C_5H_9N_2O_{n-2}\cdot][NO_2] - k_{wall}[C_5H_9N_3O_n]$$

449 where [C₅H₉N₃O_n], [C₅H₉N₂O_{n-2}•], and [NO₂] are the concentration of these species, k is the rate
450 constant and k_{wall} is the wall loss rate. Because the products of C₅H₉N₂O_{n-2}• and NO₂ were at their maximum at
451 the end of each period and decreased rapidly after isoprene addition (Fig. S8), the concentration should have its
452 maximum increasing rate at the end of each isoprene addition period. However, we found that only C₅H₉N₃O₁₂,
453 _{15, 16} showed such a time profile (Fig. S9), while C₅H₉N₃O_{9, 10, 11, 13, 14} generally increased with time, different
454 from what one would expect based on the proposed pathway. Therefore, it is likely that C₅H₉N₃O_{12, 15, 16} were
455 mainly formed via the reaction of C₅H₉N₂O_n• with NO₂, whereas C₅H₉N₃O_{9,10,11,13,14} were not. Moreover,
456 C₅H₉N₃O₉ cannot be explained by the reaction C₅H₉N₂O_n• (n≥9) with NO₂ or NO₃, because these reactions
457 would add at least one more oxygen atom. One possible pathway to form C₅H₉N₃O₉ was the direct addition of
458 N₂O₅ to the carbon double bond of C5-hydroxynitrate, forming a nitronitrate. Such a mechanism has been
459 proposed previously in the heterogeneous reaction of N₂O₅ with 1-palmitoyl-2-oleoyl-sn-glycero-3-
460 phosphocholine (POPC) because -NO₂ and -NO₃ groups were detected (Lai and Finlayson-Pitts, 1991). This
461 pathway generally matched the time series of C₅H₉N₃O_{9,10,11,13,14} typical of second-generation products since
462 C5-hydroxynitrate was a first-generation product. It is possible that the main pathway of C₅H₉N₃O_{9,10,11,13,14} was
463 the reaction of C₅H₉NO_{4,5,6} with N₂O₅, although the reaction of N₂O₅ with C=C double bonds in common alkenes
464 and unsaturated alcohols are believed to be not important (Japar and Niki, 1975; Pfrang et al., 2006).

465 3N-monomer, C₅H₉N₃O₁₀, has been observed in the particles formed in the isoprene+NO₃ reaction by
466 Ng et al. (2008). Here a complete series of C₅H₉N₃O_n were observed. C₅H₉N₃O₁₀ was previously proposed to
467 be formed by another pathway, i.e. the reaction of RO₂ (C₅H₉N₂O₉•) and NO₃ (Ng et al., 2008). We further
468 examined the possibility of such a pathway in our study. Similar to NO₂, if C₅H₉N₃O_n were formed by the
469 reaction of C₅H₉N₂O_{n-2}• with NO₃, the concentration would have its maximum increasing rate at the end of each
470 isoprene addition period. Among C₅H₉N₂O_n•, the precursors of C₅H₉N₃O_n, C₅H₉N₂O_{9, 10, 13, 14}• showed a

471 maximum increasing rate and a subsequent decrease after isoprene addition. The difference in oxygen number
 472 between $C_5H_9N_3O_{12, 15, 16}$, the termination products, and $C_5H_9N_2O_{9, 10, 13, 14}$, the corresponding RO_2 with the
 473 consistent time profile is mostly two. Since the reaction of $C_5H_9N_2O_n$ with NO_2 and NO_3 result an increased
 474 oxygen number by two and by one, respectively, we infer that it is more likely that $C_5H_9N_3O_{12, 15, 16}$ were formed
 475 by the reaction of $C_5H_9N_2O_{10, 13, 14}$ with NO_2 rather than NO_3 , and thus they were likely peroxy nitrates rather
 476 than nitrates formed by the reaction of RO_2 with NO_3 . Since alkyl peroxy nitrates decompose rapidly (Finlayson-
 477 Pitts and Pitts, 2000; Ziemann and Atkinson, 2012), it is possible that these compounds contained
 478 peroxyacylnitrates.

479 Little attention has been paid to the RO_2+NO_2 pathway in nighttime chemistry of isoprene in the
 480 literature (Wennberg et al., 2018), which is likely due to the instability of the products. According to this
 481 pathway, $C_5H_8N_2O_n$, which was proposed to be a ketone formed via $C_5H_9N_2O_9$ in the M2 series (Table 1) as
 482 discussed above, can also comprise peroxy nitrate formed by the reaction of $C_5H_8NO_n$ (M1a RO_2) with NO_2 .
 483 3N dimer such as $C_5H_9N_3O_{10}$ or have been observed in a recent field study in polluted cities in east China (Xu
 484 et al., 2021).

485 3.3 HOM dimers and their formation

486 Table 2. HOM dimers and trimers formed in the oxidation of isoprene by NO_3 .

Series Number	Formula	Type	Pathway of RO_2
Dimer 1	$C_{10}H_{16}N_2O_n$ (n=10-17)	ROOR ^a	M1 ^b + M1
Dimer 2	$C_{10}H_{17}N_3O_n$ (n=11-19)	ROOR	M1+M2/M3+M4
Dimer 3	$C_{10}H_{18}N_4O_n$ (n=15-18)	ROOR	M2+M2
Dimer 4	$C_{10}H_{18}N_2O_n$ (n=10-16)	ROOR	M1+M4
Dimer 5	$C_{10}H_{15}N_3O_n$ (n=13-17)	ROOR	M1+M3
Dimer 6	$C_{10}H_{19}N_3O_n$ (n=14-15)	ROOR	M2+M4
Dimer 7	$C_{10}H_{14}N_2O_n$ (n=10-16)	ROOR	Unknown
Dimer 8	$C_{10}H_{15}NO_n$ (n=9-12)	ROOR	$C_{10}H_{16}NO_n$
Dimer 9	$C_{10}H_{17}NO_n$ (n=9-15)	ROOR	$C_{10}H_{16}NO_n$
Dimer R1	$C_{10}H_{16}N_3O_n$ (n=12-15)	RO_2	Dimer 1+ NO_3
Dimer R2	$C_{10}H_{17}N_2O_n$ (n=11-12)	RO_2	Dimer 1+OH
Dimer R3	$C_{10}H_{17}N_4O_n$ (n=16-18)	RO_2	Dimer 2+ NO_3
Dimer R4	$C_{10}H_{16}NO_n$ (n=10-14)	RO_2	M1+ C_5H_8
Trimer 1	$C_{15}H_{24}N_4O_n$ (n=17-22)	ROOR	Dimer R1+M1
Trimer 2	$C_{15}H_{25}N_5O_n$ (n=20-22)	ROOR	Dimer R3+M1; Dimer R1+M2
Trimer 3	$C_{15}H_{25}N_3O_n$ (n=13-20)	ROOR	Dimer R2+M1; Dimer R4+M2
Trimer 4	$C_{15}H_{26}N_4O_n$ (n=17-21)	ROOR	Dimer R2+M2

487 ^a: ROOR denotes for organic peroxide.

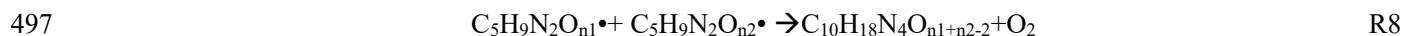
488 ^b: The numbering is referred to Table 1.

489 A number of HOM dimer series were observed, including $C_{10}H_{16}N_2O_n$ (n=10-17), $C_{10}H_{17}N_3O_n$ (n=11-19), and
 490 $C_{10}H_{18}N_4O_n$ (n=15-18), $C_{10}H_{18}N_2O_n$ (n=10-16), $C_{10}H_{15}N_3O_n$ (n=13-17), and $C_{10}H_{19}N_3O_n$ (n=14-15) series (Table 2,

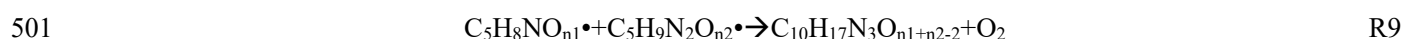
491 Table S3). $C_{10}H_{16}N_2O_n$ series (dimer 1, Table 2) was likely formed by the accretion reaction of two monomer RO_2
 492 of M1a/b (Reaction R7).



494 Similarly, $C_{10}H_{18}N_4O_n$ series (dimer 2, Table 2) were likely formed by the accretion reaction of two monomer RO_2
 495 of M2 (Reaction R8). As n_1 and n_2 are ≥ 9 , the number of oxygen in $C_{10}H_{18}N_4O_n$ is expected to be ≥ 16 . This is
 496 consistent with our observation that only $C_{10}H_{18}N_4O_n$ with $n \geq 16$ had significant concentrations.

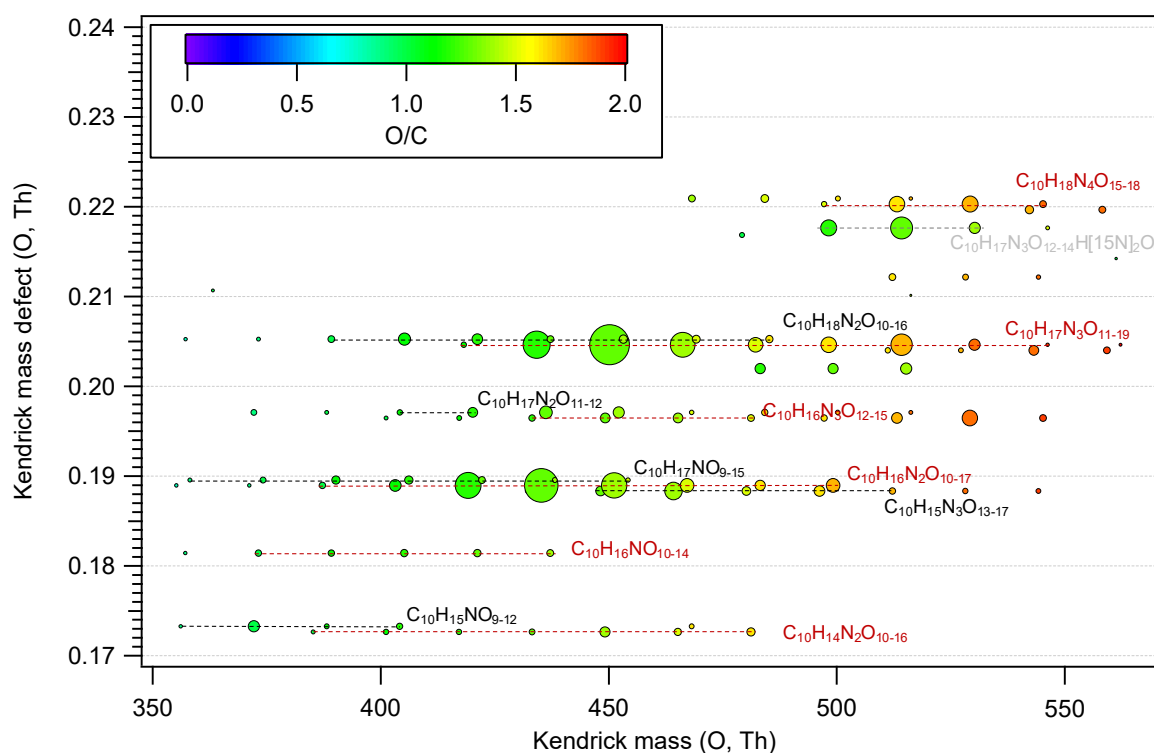


498 $C_{10}H_{17}N_3O_n$ series (dimer 3, Table 2) were likely formed by the cross accretion reaction of one M1 RO_2 and one
 499 M2 RO_2 (reaction R9). Since n_1 is ≥ 5 and n_2 is ≥ 9 , the number of oxygen atoms in $C_{10}H_{17}N_3O_n$ is expected to be
 500 ≥ 12 , which is also roughly consistent with our observation that only $C_{10}H_{17}N_3O_n$ with $n \geq 11$ were detected.



502 Similarly, $C_{10}H_{18}N_2O_n$ ($n=10-16$) and $C_{10}H_{15}N_3O_n$ ($n=13-17$) series (dimer 4, dimer 5, Table 2) were likely formed
 503 from the accretion reaction between one M1 RO_2 and one M4 RO_2 , and between one M1 RO_2 and one M3 RO_2
 504 ($C_5H_7N_2O_9\bullet$). Other dimer series than dimer 1-5 were also present. However, they had quite low intensity (Fig. 4),
 505 which was consistent with the low abundance of their parent monomer RO_2 . They can be formed from various
 506 accretion reactions of monomer RO_2 . For example, $C_{10}H_{19}N_3O_n$ can be formed by the accretion reaction of
 507 $C_5H_9N_2O_n\bullet$ and $C_5H_{10}NO_n\bullet$ (Table 2).

508 Similar to monomers, a few species dominated in HOM dimers spectrum. The dominant dimer series were
 509 $C_{10}H_{17}N_3O_x$ and $C_{10}H_{16}N_2O_x$ series, with $C_{10}H_{17}N_3O_{12-14}$ and $C_{10}H_{16}N_2O_{12-14}$ showing highest intensity among each
 510 series (Fig. 4). In addition, the O/C ratio or oxidation state of HOM dimers were generally lower than that of
 511 monomers (Fig. 2, Fig. 4), which resulted from the loss of two oxygen atoms in the accretion reaction of two
 512 monomer RO_2 .



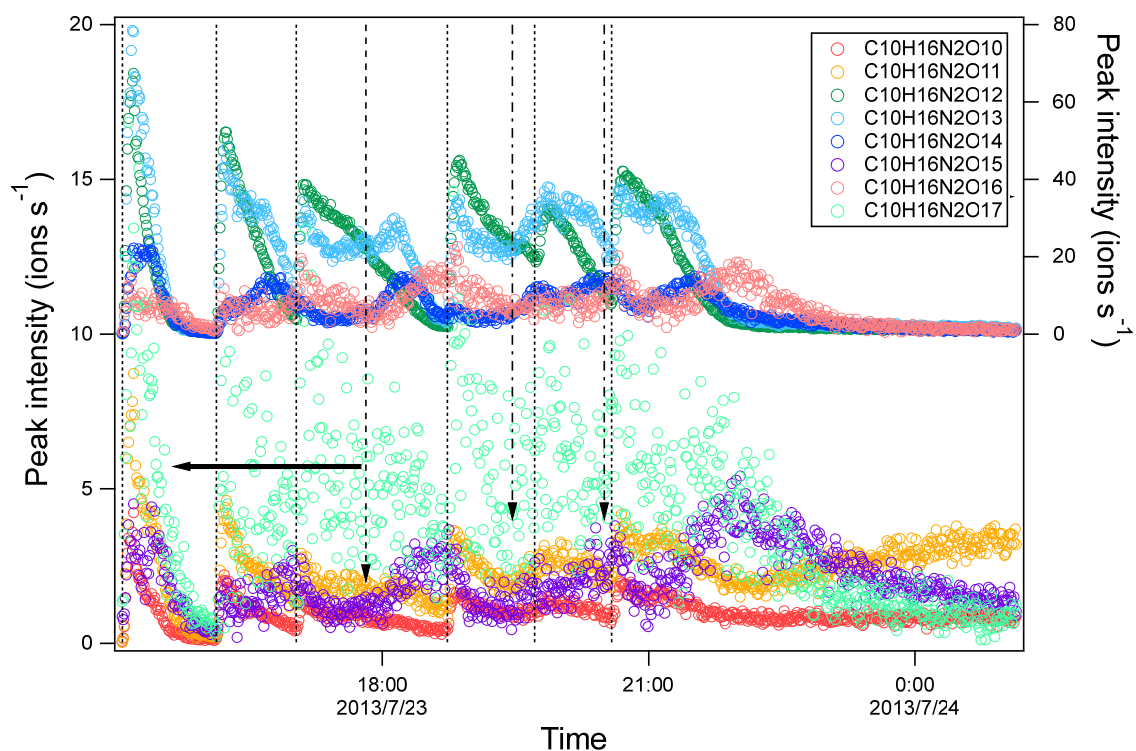
513

514 Figure 4. Kendrick mass defect plot for O of HOM dimers formed in the isoprene+NO₃ reaction. The size (area)
515 of circles is set to be proportional to the average peak intensity of each molecular formula during the first isoprene addition
516 period (P1). The molecular formula include the reagent ion ¹⁵NO₃⁻, which is not shown for simplicity. The species
517 labelled in grey (C₁₀H₁₇N₃O₁₂₋₁₄ H[¹⁵N]₂O₆⁻) are the adducts of C₁₀H₁₇N₃O₁₂₋₁₄ with H[¹⁵N]₂O₆⁻.

518 According to the mechanism above (R7-9), we attempt to explain the relative intensities of the dimers using
519 the signal intensities of monomer RO₂. Assuming that the rate constant for each of HOM-RO₂+ HOM-RO₂ reaction
520 forming dimers is the same considering that all HOM-RO₂ are highly oxygenated with a number of functional groups,
521 it is expected that the dimer formed by the recombination between the most abundant RO₂ has the highest intensity.
522 The most abundant monomer RO₂ were C₅H₉N₂O₉[•] and C₅H₉N₂O₁₀[•] and thus the most abundant dimers are expected
523 to be C₁₀H₁₆N₄O₁₆, C₁₀H₁₆N₄O₁₇, and C₁₀H₁₆N₄O₁₈. This expected result is in contrast with our observation showing
524 that the most abundant dimers were C₁₀H₁₇N₃O₁₂₋₁₄ and C₁₀H₁₆N₂O₁₂₋₁₄ (Fig. 4). The discrepancy is possibly
525 attributed to the presence of less oxygenated RO₂ (with O≤5) that have a low detection sensitivity in the NO₃-CIMS
526 (Riva et al., 2019) due to their lower oxygenation compared with other HOM RO₂ shown above. These RO₂ may
527 react with C₅H₉N₂O₉[•] and C₅H₉N₂O₁₀[•]. For example, C₅H₈NO₅[•] (RO₂) is proposed to be an important first-
528 generation RO₂ in the oxidation of isoprene by NO₃ (Ng et al., 2008; Rollins et al., 2009; Kwan et al., 2012;
529 Schwantes et al., 2015). Although C₅H₈NO₅[•] showed very low signal in our mass spectra, it was likely to have high
530 abundance since it was the first RO₂ formed in the reaction of isoprene with NO₃. Indeed, we found that the
531 termination products of C₅H₈NO₅[•] such as C₅H₉NO₅, C₅H₇NO₄, and C₅H₉NO₄ had high abundance in another study,
532 indicating the high abundance of C₅H₈NO₅[•]. The accretion reaction of C₅H₈NO₅[•] with C₅H₉N₂O₉₋₁₀[•] and C₅H₈NO₉₋₁₀[•]
533 can explain the high abundance of C₁₀H₁₇N₃O₁₂₋₁₄ and C₁₀H₁₆N₂O₁₂₋₁₄ among all dimers.

534 Provided that C₅H₈NO₅[•] is abundant, we still cannot explain the relative intensity of C₁₀H₁₇N₃O₁₂,
535 C₁₀H₁₇N₃O₁₃, and C₁₀H₁₇N₃O₁₄ that were all formed by the accretion reaction with C₅H₈NO₅[•]. C₁₀H₁₇N₃O₁₂ should
536 have the highest intensity among C₁₀H₁₇N₃O₁₂₋₁₄ as its precursor RO₂, C₅H₉N₂O₉[•], is the most abundant. This
537 suggests that accretion reactions other than those of C₅H₈NO₅[•] with C₅H₉N₂O₉₋₁₀[•] also contributed to C₁₀H₁₇N₃O₁₂₋₁₄.
538 Admittedly, the assumption of different RO₂ having similar rate constants in accretion reactions may not be valid.
539 For example, self-reaction of tertiary RO₂ is slower than secondary and primary RO₂ (Jenkin et al., 1998; Finlayson-
540 Pitts and Pitts, 2000). Different rate constants may also lead to the observation that the most abundant dimers could
541 not be explained the most abundant RO₂.

542



543

544 Figure 5. Time series of peak intensity of several HOM dimers of $C_{10}H_{16}N_2O_n$ series. The dashed lines
 545 indicate the time of isoprene additions. The long-dashed arrow indicates the time of NO_2 addition. The dash-dotted
 546 arrows indicate the time of O_3 additions. The horizontal arrows indicate y-axis scales for different markers.

547

548 The time profiles of $C_{10}H_{16}N_2O_n$ indicate contributions of both the first- and second-generation products.
 549 The dominance of the first- or second-generation products depended on the specific compounds. Most $C_{10}H_{16}N_2O_n$
 550 compounds increased instantaneously after isoprene additions, indicating significant contributions of first-generation
 551 products. Since the formation of $C_{10}H_{16}N_2O_n$ likely involved $C_5H_8NO_5^\bullet$ as discussed above, the instantaneous
 552 increase may result from the increase of $C_5H_8NO_5^\bullet$ as well as other first-generation RO_2 . After the initial increase,
 553 $C_{10}H_{16}N_2O_{10-12}$ then decayed with time (Fig. 5) while $C_{10}H_{16}N_2O_{13-15}$ increased again in the later phase of a period
 554 and when NO_2 and O_3 were added. The second increase indicated that $C_{10}H_{16}N_2O_{13-15}$ may contain more than one
 555 isomer, which had different production pathways. As discussed above, $C_5H_8NO_n^\bullet$ can be either a first-generation
 556 RO_2 formed directly via the reaction of isoprene with NO_3 and autoxidation, or a second-generation RO_2 , e.g. formed
 557 via the reaction of with $C_5H_8O_2$ with NO_3 . Therefore the second increase of $C_{10}H_{16}N_2O_{13-15}$ may result from the
 558 reaction of two first-generation RO_2 and of two second-generation RO_2 or between one first-generation and one
 559 second-generation RO_2 . The increase of $C_{10}H_{16}N_2O_{14-15}$ after isoprene addition was not large, indicating the
 560 larger contributions from second-generation products compared with other $C_{10}H_{16}N_2O_n$. Overall, as the number
 561 of oxygen increased, the contribution of second-generation products to $C_{10}H_{16}N_2O_n$ increased.

561

562 In contrast to $C_{10}H_{16}N_2O_n$ series, $C_{10}H_{18}N_4O_n$ increased gradually after each isoprene addition and then
 563 decreased afterward (Fig. 6), either naturally or after isoprene additions, which is typical for second-generation
 564 products. Since $C_{10}H_{18}N_4O_n$ was likely formed by the accretion reaction of $C_5H_9N_2O_n^\bullet$ (RO_2), the time profile
 of $C_{10}H_{18}N_4O_n$ was as expected since $C_5H_9N_2O_n^\bullet$ was formed via the reaction of NO_3 with first-generation

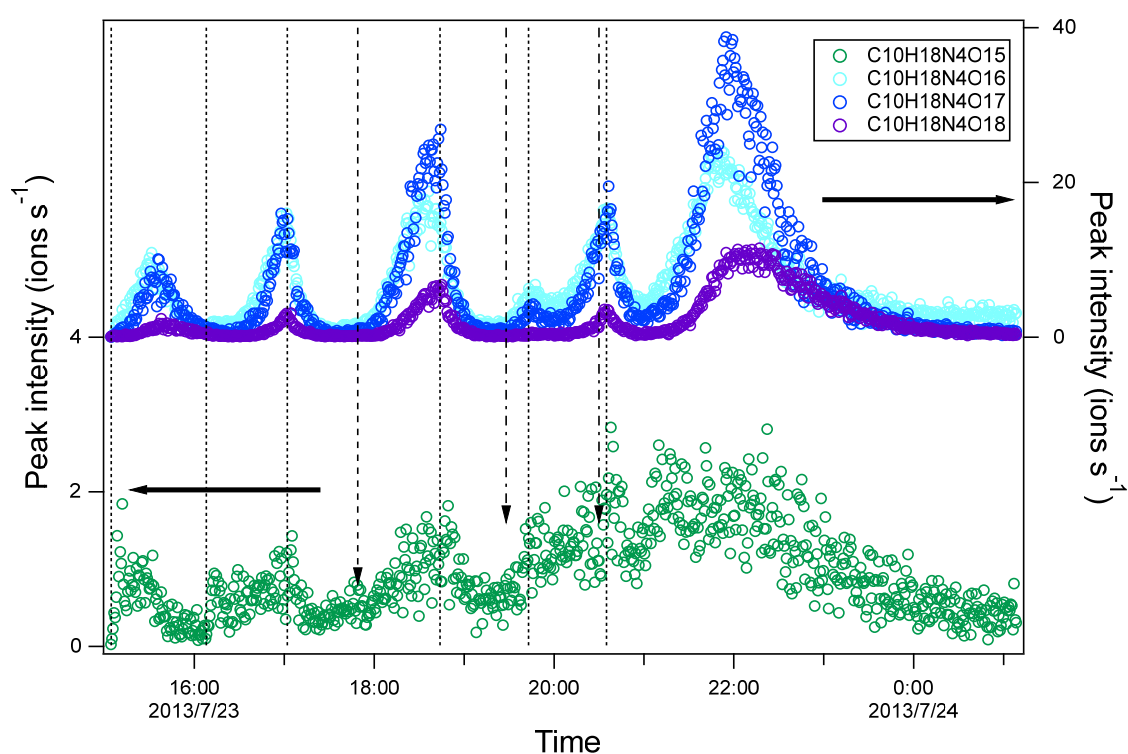
565 products $C_5H_9NO_n$. The $C_{10}H_{18}N_4O_n$ concentration depended on the product of the concentrations of two
 566 $C_5H_9N_2O_n$. Taking $C_{10}H_{18}N_4O_{16}$ as an example, its concentration can be expressed as follows:

$$567 \quad \frac{d[C_{10}H_{18}N_4O_{16}]}{dt} = k[C_5H_9N_2O_9][C_5H_9N_2O_9] - k_{wl}[C_{10}H_{18}N_4O_{16}]$$

568 When the concentration of $C_5H_9N_2O_9$ increased, the changing rate of $C_{10}H_{18}N_4O_{16}$ was positive and increased
 569 and thus the concentration of $C_{10}H_{18}N_4O_{16}$ increased. When the concentration $C_5H_9N_2O_9$ decreased sharply
 570 after isoprene additions, the changing rate of $C_{10}H_{18}N_4O_{16}$ decreased and even became negative values, and thus
 571 the concentration of $C_{10}H_{18}N_4O_{16}$ decreased after isoprene addition.

572 Similar to the $C_{10}H_{16}N_2O_n$ series, while $C_{10}H_{17}N_3O_n$ first increased instantaneously with isoprene
 573 addition, it increased again during the later stage of each period (Fig. S10), showing a mixed behavior of the
 574 first-generation products and second-generation products. The time series of $C_{10}H_{17}N_3O_n$ was as expected in
 575 general because $C_{10}H_{17}N_3O_n$ was likely formed via the accretion reaction of $C_5H_8NO_n$ (M1 RO₂) and
 576 $C_5H_9N_2O_n$ (M2 RO₂), which were first- or second-generation, and second-generation RO₂, respectively.

577

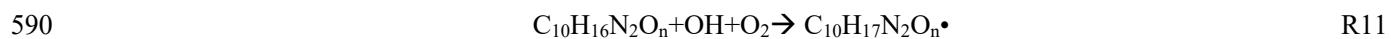


578

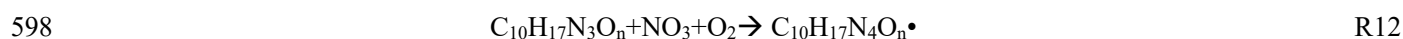
579 Figure 6. Time series of peak intensity of several HOM dimers of $C_{10}H_{18}N_4O_n$ series. The dashed lines indicate the
 580 time of isoprene additions. The long-dashed arrow indicates the time of NO_2 addition. The dash-dotted arrows
 581 indicate the time of O_3 additions. The horizontal arrows indicate y-axis scales for different markers.

582 Some dimers that cannot be explained by accretion reactions such as $C_{10}H_{16}N_3O_n$ ($n=12-15$), $C_{10}H_{17}N_2O_n$ ($n=11-$
 583 12), $C_{10}H_{16}NO_n$ ($n=10-14$), $C_{10}H_{15}NO_n$ ($n=9-12$), $C_{10}H_{17}NO_n$ ($n=9-15$) were also observed. These dimers had low abundance.
 584 We note that due to their low signals in the mass spectra, their assignment and thus range of n may be subject to
 585 uncertainties. Since $C_{10}H_{16}NO_n$ ($n=10-16$), $C_{10}H_{16}N_3O_n$ ($n=12-15$), and $C_{10}H_{17}N_2O_n$ contain unpaired electrons, they

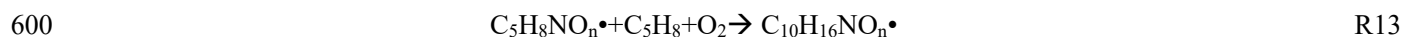
586 cannot be formed via the direct accretion reaction of two RO₂. Instead, C₁₀H₁₆N₃O_n (n=12-15) • (dimer R1) and
587 C₁₀H₁₇N₂O_n • (dimer R2) were likely RO₂ formed by the reaction of HOM dimers containing a double bond (dimer
588 1) with NO₃ and with OH, respectively, followed by the reaction with O₂.



591 The corresponding termination products of C₁₀H₁₆N₃O_n • RO₂ series such as C₁₀H₁₅N₃O_n (ketone), C₁₀H₁₇N₃O_n
592 (hydroperoxide/alcohol) were also observed, although these compounds can also be formed via reactions between
593 two RO₂ radicals (R9 and R11). Among the termination products, C₁₀H₁₅N₃O_n had low intensity. Reaction R13 and
594 the termination reaction of C₁₀H₁₇N₂O_n • with HO₂ provided an additional pathway to C₁₀H₁₇N₃O_n besides the R9
595 pathway discussed above. Similarly, other dimers may also be formed by the termination reactions of dimer RO₂
596 with RO₂ or HO₂. E.g., C₁₀H₁₈N₄O_n can be formed via termination reaction of C₁₀H₁₇N₄O_n • with another RO₂ wherein
597 C₁₀H₁₇N₄O_n • can be formed as follows:



599 C₁₀H₁₆NO_n (n=10-14) • could be explained by the reaction of monomer RO₂ with isoprene.



601 Only C₁₀H₁₆NO_n • with n ≥ 10 were detected, while according to the mechanism of self-reaction between C₅H₈NO_n •,
602 the n range of C₁₀H₁₆NO_n • is expected to be 7-14. The absence of C₁₀H₁₆NO_n (n < 10) • is likely attributed to their low
603 abundance, which might result from low precursor concentrations, low reaction rates with isoprene, and/or faster
604 reactive losses with other radicals. Such a reaction of RO₂ with isoprene has been proposed by Ng et al. (2008) and
605 Kwan et al. (2012). The corresponding termination products of C₁₀H₁₆NO_n • are C₁₀H₁₅NO_n (ketone) and C₁₀H₁₇NO_n
606 species (hydroperoxide/alcohol). C₁₀H₁₇NO_n species showed a time profile of typical first-generation products (Fig.
607 S11), i.e. increasing immediately with isoprene addition and then decaying with time. This behaviour further supports
608 the possibility of reaction R13. Yet, the reaction rate of alkene with RO₂ is likely low due to the high activation
609 energy (Stark, 1997, 2000). It is worth noting that to our knowledge no experimental kinetic data on the addition of
610 RO₂ to alkenes in the gas phase in atmospheric relevant conditions are available, though fast, low-barrier ring closure
611 reactions in unsaturated RO₂ radicals have been reported (Vereecken and Peeters, 2004, 2012; Kaminski et al., 2017;
612 Richters et al., 2017; Chen et al., 2021). We would like to note that there is unlikely interference to C₁₀-HOM from
613 monoterpenes, which has been reported previously (Bernhammer et al., 2018), as the concentration of monoterpenes
614 in the chamber during this study was below the limit of detection, which was ~50 ppt (3σ).

615 Some of the dimers discussed above have been observed in previous laboratory studies. Ng et al. (2008)
616 found C₁₀H₁₆N₂O₈ and C₁₀H₁₆N₂O₉ in the gas phase and C₁₀H₁₇N₃O₁₂, C₁₀H₁₇N₃O₁₃, C₁₀H₁₈N₄O₁₆, and C₁₀H₁₇N₅O₁₈
617 in the particle phase. C₁₀H₁₆N₂O₈ and C₁₀H₁₆N₂O₉ were also observed in our study, but their intensity in the MS was
618 too low to assign molecular formulas with high confidence. The low intensity may be due to the low sensitivity of
619 C₁₀H₁₆N₂O_{8,9} in NO₃⁻-CIMS. According to modelling results of the products formed in cyclohexene ozonolysis by
620 Hyttinen et al. (2015), at least two hydrogen bond donor functional groups are needed for a compound to be detected
621 in a nitrate CIMS. As C₁₀H₁₆N₂O₈ and C₁₀H₁₆N₂O₉ have no and only one H-bond donor function groups, respectively,
622 they are expected to have low sensitivity in NO₃⁻-CIMS. Moreover, the low intensity can be partly attributed to the
623 much lower isoprene concentrations used in this study compared to previous studies, leading to the low concentration

624 of C₁₀H₁₆N₂O₈ and C₁₀H₁₆N₂O₉ (Ng et al., 2008). C₁₀H₁₇N₃O₁₂, C₁₀H₁₇N₃O₁₃, C₁₀H₁₈N₄O₁₆, and C₁₀H₁₇N₅O₁₈ were
625 all observed in the gas phase in this study, wherein the concentration of C₁₀H₁₇N₅O₁₈ was very low. The formation
626 pathways of C₁₀H₁₇N₃O₁₂, C₁₀H₁₇N₃O₁₃, and C₁₀H₁₈N₄O₁₆ (R8) were generally similar to those proposed by Ng et al.
627 (2008) except that the products from H-shift of RO₂ were involved in the formation of C₁₀H₁₇N₃O₁₃. Among the two
628 pathways of C₁₀H₁₈N₄O₁₆ formation (R8 and via R12), our results indicate that R8 was the main pathway, based on
629 the low concentrations of C₁₀H₁₇N₄O_{16/17}• and other termination product of them, C₁₀H₁₆N₄O_{15/16}. That the time
630 profile of C₁₀H₁₈N₄O₁₆ was consistent with what is expected from R8 as discussed above offers additional evidence
631 to that conclusion.

632 Few field studies have reported HOM dimers formed via the reaction NO₃ with isoprene. This might be
633 because NO₃+isoprene-HOM dimers can have the identical molecular formula to the HOM monomers from
634 monoterpene oxidation. Possible contribution of dimer formation in the isoprene oxidation to C₆-10 HOM in the
635 particle phase observed at a rural site Yorkville, US is reported by Chen et al. (2020), although these HOM are
636 attributed to be more likely from monoterpene oxidation.

637 3.4 HOM trimers and their formation

638 A series of HOM trimers were observed, such as C₁₅H₂₄N₄O_n (n=17-22), C₁₅H₂₅N₅O_n (n=20-22), C₁₅H₂₅N₃O_n
639 (n=13-20), C₁₅H₂₆N₄O_n (n=17-21), and C₁₅H₂₄N₂O_n (n=12-16). Among the trimers, C₁₅H₂₄N₄O_n was the most abundant series
640 (Fig. S12). The C₁₅H₂₄N₄O_n series can be explained by the accretion reaction of one monomer HOM RO₂ and
641 one dimer HOM RO₂.



643 The formation pathways of dimer RO₂ C₁₀H₁₆N₃O_n (n=12-15) and C₁₀H₁₇N₂O_n are shown above (reaction R10 and
644 R11).

645 The other trimers were likely formed via similar pathways (Table 2 and Supplement S2). Since NO₃⁻-CIMS
646 cannot provide the structural information of these HOM trimers, we cannot elucidate the major pathways. However,
647 in all these pathways, dimer-RO₂ is necessary to form a trimer, and most of the dimer-RO₂ formation pathways
648 require at least one double bond in the dimer molecule except for the reaction of RO₂ with isoprene. Since one
649 double bond has already reacted in the monomer-RO₂ formation, we anticipate that in the reaction with NO₃ it is
650 more favourable for precursors (VOC) containing more than one double bonds to form trimer molecules than
651 precursors containing only one double bond, as it is easier to generate new RO₂ radicals from these dimers by
652 attack on the remaining double bond(s).

653 The time profile of C₁₅H₂₄N₄O_n showed the mixed behavior of first- and second-generation products (Fig.
654 S13), consistent with the mechanism discussed above since C₅H₈NO_n• and C₁₀H₁₆N₃O_n• were of first- or second-
655 generation and second-generation, respectively. The contributions of the second-generation products became
656 larger as the number of oxygen atoms increased. In contrast, C₁₅H₂₅N₃O_n showed instantaneous increase with
657 isoprene addition (Fig. S14), which was typical for time profiles of first-generation products. Both proposed
658 formation pathways of C₁₅H₂₅N₃O_n (RS6 and RS7) contained a second-generation RO₂, which was not in line with
659 the time profile observed. The observation cannot be well explained, unless we assume molecular adducts of a dimer

660 with one monomer. It is also possible that some $C_{10}H_{17}N_2O_n\bullet$ were formed very fast or that there were other
661 formation pathways of $C_{15}H_{25}N_3O_n$ not accounted for here.

662 We are not aware of field studies reporting NO_3 +isoprene-HOM trimers, which is likely due to the same
663 reason for dimers discussed above. It is challenging to distinguish HOM trimers formed in the reaction NO_3 with
664 isoprene from the dimers formed by cross reaction of the RO_2 from monoterpene oxidation ($C_{10}-RO_2$) with that from
665 isoprene oxidation (C_5-RO_2) as their molecular formula can be identical.

666 3.5 Contributions of monomers, dimer, and trimers to HOM

667 The concentration (represented by peak intensity) of monomers was higher than that of dimers, but overall
668 their concentrations remained of the same order of magnitude (Fig 1a, inset). The concentration of trimers was much
669 lower than that of monomers and dimers. The relative contributions of monomers, dimers, and trimers evolved in
670 time due to the changing concentration of each HOM species. Comparing the contributions of various classes of
671 HOM in period 1 with those in periods 1-6 reveals that the relative contribution of monomers increased with time,
672 especially that of 2N-monomers, while the contribution of dimers decreased. This trend is attributed to the larger wall
673 loss of dimers compared to monomers because of their lower volatility and also to the continuous formation of
674 second-generation monomers, mostly 2N-monomers. Overall, the relative contribution of total HOM monomers
675 decreased immediately after isoprene addition while the contribution of HOM dimers increased rapidly (Fig. S15),
676 which was attributed to the faster increase of dimers intensity due to their rapid formation. Afterwards, the
677 contribution of monomers to total HOM gradually increased and that of dimers decreased, which was partly due to
678 the faster wall loss rate of dimers and to the continuous formation of second-generation monomers.

679 3.6 Yield of HOM

680 The HOM yield in the oxidation of isoprene by NO_3 was estimated using the sensitivity of H_2SO_4 . It was
681 derived for the first isoprene addition period to minimize the contribution of multi-generation products and to better
682 compare with the data in literature, thus denoted as primary HOM yield (Pullinen et al., 2020) and was estimated to
683 be $1.2\%_{-0.7\%}^{+1.3\%}$. The uncertainty was estimated as shown in the Supplement S1. Despite the uncertainty, the primary
684 HOM yield here was much higher than the HOM yield from the ozonolysis and photooxidation of isoprene (Jokinen
685 et al., 2015). The difference may be attributed to the more efficient oxygenation in the addition of NO_3 to carbon
686 double bonds. Compared with the reaction with O_3 or OH, the initial peroxy radicals contains 5 oxygen atoms when
687 isoprene reacts with NO_3 , while the initial peroxy radicals contains only 3 oxygen atoms when reacting with OH, and
688 the ozonide contains 3 oxygen atoms in the case of O_3 .

689 4 Conclusion and implications

690 HOM formation in the reaction of isoprene with NO_3 was investigated in the SAPHIR chamber. A number
691 of HOM monomers, dimers, and trimers containing one to five nitrogen atoms were detected, and their time-
692 dependent concentration profiles were tracked throughout the experiment. Some formation mechanisms for various
693 HOM were proposed according to the molecular formula identified, and the available literature. HOM showed a
694 variety of time profiles with multiple isoprene additions during the reaction. First-generation HOM increased

695 instantaneously after isoprene addition and then decreased while second-generation HOM increased gradually and
696 then decreased with time, reaching a maximum concentration at the later stage of each period. The time profiles
697 provide additional constraints on their formation mechanism beside the molecular formula, suggesting whether they
698 were first-generation products or second-generation products or a combination of both. 1N-monomers (mostly C₅)
699 were likely formed by NO₃ addition to a double bond of isoprene, forming monomer RO₂, followed by autoxidation
700 and termination via the reaction with HO₂, RO₂, and NO₃. Time series suggest that some 1N-monomer could also be
701 formed by the reaction of first-generation products with NO₃, and thus be of second-generation. 2N-monomers were
702 likely formed via the reaction of first-generation products such as C₅-hydroxynitrate with NO₃ and thus second-
703 generation products. 3N-monomers likely comprised peroxy/peroxyacyl nitrates formed by the reaction of 2N-
704 monomer RO₂ with NO₂, and possibly nitronitrates formed via the direct addition of N₂O₅ to the first-generation
705 products. HOM dimers were mostly formed by the accretion reactions between various HOM monomer RO₂, either
706 first-generation or second-generation or with the contributions of both, and thus showed time profiles typical of either
707 first-generation products, or second-generation products, or a combination of both. Additionally, some dimers peroxy
708 radicals (dimer RO₂) were formed by the reaction of NO₃ with dimers containing a C=C double bond. HOM trimers
709 were proposed to be formed by accretion reactions between the monomer RO₂ and dimer RO₂.

710 Overall, both HOM monomers and dimers contribute significantly to total HOM while trimers only
711 contributed a minor fraction. Within both the monomer and dimer compounds, a limited set of compounds dominated
712 the abundance, such as C₅H₈N₂O_n, C₅H₁₀N₂O_n, C₁₀H₁₇N₃O_n, and C₁₀H₁₆N₂O_n series. 2N-monomers, which were
713 second-generation products, dominated in monomers and accounted for ~34% of all HOM, indicating the important
714 role of second-generation oxidation in HOM formation in the isoprene+NO₃ reaction. Both RO₂ autoxidation and
715 “alkoxy-peroxy” pathways were found to be important for 1N- and 2N-HOM formation. In total, the yield of HOM
716 monomers, dimers, and trimers accounted for 1.3%^{+1.3%}_{-0.7%} of the isoprene reacted, which was much higher than the HOM
717 yield in the oxidation of isoprene by OH and O₃ reported in the literature (Jokinen et al., 2015). This means that the
718 reaction of isoprene with NO₃ is a competitive pathway of HOM formation from isoprene.

719 The HOM in the reaction of isoprene with NO₃ may account for a significant fraction of SOA. If all the
720 HOM condense on particles, using the molecular weight of the HOM with the least molecular weight observed in
721 this study (C₅H₉NO₆), the HOM yield corresponds to a SOA yield of 3.6%. Although SOA concentrations were not
722 measured in this study, Ng et al. (2008) reported a SOA yield of the isoprene+NO₃ reaction of 4.3%-23.8%. Rollins
723 et al. (2009) reported a SOA yield of 2% at low organic aerosol loading (~0.52 μg m⁻³) and 14% if the further
724 oxidation of the first-generation products are considered in the isoprene+NO₃ reaction. Comparing the potential
725 SOA yield produced by HOM with SOA yields in the literature suggests that HOM may play an important role in the
726 SOA formation in the isoprene+NO₃ reaction.

727 The RO₂ lifetime is approximately 20-50 s in our experiments, which is generally comparable or shorter than
728 the lifetime of RO₂ in the ambient atmosphere at night, varying from several 10 s to several 100 s (Fry et al., 2018),
729 depending on the NO₃, HO₂, and RO₂ concentrations. Assuming a HO₂, RO₂, and NO₃ concentration of 5 ppt, 5 ppt
730 (Tan et al., 2019), and 300 ppt (Brown and Stutz, 2012) respectively, the RO₂ lifetime in our study is comparable to
731 the nighttime RO₂ lifetime (50 s) found in urban locations and areas influenced by urban plume. In areas with longer
732 RO₂ lifetime such as remote areas, the autoxidation is expected to be more important relative to bimolecular reactions.

733 This may enhance HOM yield and thus enhance SOA yield. However, on the other hand, at lower RO₂ concentration
734 and thus longer RO₂ lifetime, reduced rates of RO₂+RO₂ reactions producing low-volatility dimers can reduce the
735 SOA yield via reducing dimer yield (McFiggans et al., 2019; Pullinen et al., 2020). The RO₂ fate in our experiments
736 is dominated the reaction RO₂+NO₃ with significant contribution of RO₂+RO₂, which can also represent the RO₂ fate
737 in the urban areas and areas influenced by urban plume. Our experiment condition cannot represent the chemistry in
738 HO₂-dominated regions such as clean forest environment (Schwantes et al., 2015).

739 We observed the second-generation products formed by the reaction of first-generation products. The
740 lifetime of first-generation nitrates in the ambient atmosphere, according their rate constants with OH and NO₃
741 (Wennberg et al., 2018), are ~5 h and ~1.3-4 h, respectively, with respect to the reaction with OH and NO₃ assuming
742 a typical OH concentration of 2×10⁶ molecules cm⁻³ (Lu et al., 2014; Tan et al., 2019) and NO₃ concentration of 100-
743 300 ppt in urban areas (Brown and Stutz, 2012). Therefore, they have the chance to react further with OH and NO₃
744 at dawn. In our experiments, the lifetimes of these first-generation nitrates with respect to OH and NO₃ are
745 comparable to the aforementioned lifetime due to comparable OH and NO₃ concentrations with these ambient
746 conditions. Therefore, our findings on the second-generation products are relevant to the ambient urban atmosphere
747 and areas influenced by urban plumes. Some of these products such as C₅H_{8,10}N₂O₈ and multi-generation
748 nitrooxyorganosulfates have been observed in recent field studies in polluted megacities in east China (Hamilton et
749 al., 2021; Xu et al., 2021).

750 **Data availability**

751 All the data in the figures of this study are available upon request to the corresponding author (t.mentel@fz-juelich.
752 de or dfzhao@fudan.edu.cn).

753 **Competing interests**

754 The authors declare that they have no conflict of interest.

755 **Author contribution**

756 TFM, HF, SS, DZ, IP, AW, and AKS designed the experiments. Instrument deployment and operation were carried
757 out by IP, HF, SS, IA, RT, FR, DZ, and RW. Data analysis was done by DZ, HF, SS, RW, IA, RT, FR, YG, SK. DZ,
758 TFM, RW, JW, SK, and LV interpreted the compiled data set. DZ and TFM wrote the paper. All co-authors discussed
759 the results and commented on the paper.

760 **Acknowledgements**

761 We thank the SAPHIR team for supporting our measurements and providing helpful data. D. Zhao and Y. Guo would
762 like to thank the support of National Natural Science Foundation of China (41875145). We would like to thank three
763 anonymous reviewers and Kristian Møller for their helpful comments.

References

- Atkinson, R., Baulch, D. L., Cox, R. A., Crowley, J. N., Hampson, R. F., Hynes, R. G., Jenkin, M. E., Rossi, M. J., and Troe, J.: Evaluated kinetic and photochemical data for atmospheric chemistry: Volume II - gas phase reactions of organic species, *Atmos. Chem. Phys.*, 6, 3625-4055, 2006.
- Ayres, B. R., Allen, H. M., Draper, D. C., Brown, S. S., Wild, R. J., Jimenez, J. L., Day, D. A., Campuzano-Jost, P., Hu, W., de Gouw, J., Koss, A., Cohen, R. C., Duffey, K. C., Romer, P., Baumann, K., Edgerton, E., Takahama, S., Thornton, J. A., Lee, B. H., Lopez-Hilfiker, F. D., Mohr, C., Wennberg, P. O., Nguyen, T. B., Teng, A., Goldstein, A. H., Olson, K., and Fry, J. L.: Organic nitrate aerosol formation via NO_3 + biogenic volatile organic compounds in the southeastern United States, *Atmos. Chem. Phys.*, 15, 13377-13392, 10.5194/acp-15-13377-2015, 2015.
- Berndt, T., and Böge, O.: Gas-phase reaction of NO_3 radicals with isoprene: a kinetic and mechanistic study, *Int. J. Chem. Kinet.*, 29, 755-765, 10.1002/(sici)1097-4601(1997)29:10<755::Aid-kin4>3.0.Co;2-I, 1997.
- Berndt, T., Mender, B., Scholz, W., Fischer, L., Herrmann, H., Kulmala, M., and Hansel, A.: Accretion Product Formation from Ozonolysis and OH Radical Reaction of α -Pinene: Mechanistic Insight and the Influence of Isoprene and Ethylene, *Environ. Sci. Technol.*, 52, 11069-11077, 10.1021/acs.est.8b02210, 2018a.
- Berndt, T., Scholz, W., Mentler, B., Fischer, L., Herrmann, H., Kulmala, M., and Hansel, A.: Accretion Product Formation from Self- and Cross-Reactions of RO_2 Radicals in the Atmosphere, *Angew. Chem.-Int. Edit.*, 57, 3820-3824, 10.1002/anie.201710989, 2018b.
- Bernhammer, A. K., Fischer, L., Mentler, B., Heinritzi, M., Simon, M., and Hansel, A.: Production of highly oxygenated organic molecules (HOMs) from trace contaminants during isoprene oxidation, *Atmos. Meas. Tech.*, 11, 4763-4773, 10.5194/amt-11-4763-2018, 2018.
- Bianchi, F., Kurten, T., Riva, M., Mohr, C., Rissanen, M. P., Roldin, P., Berndt, T., Crouse, J. D., Wennberg, P. O., Mentel, T. F., Wildt, J., Junninen, H., Jokinen, T., Kulmala, M., Worsnop, D. R., Thornton, J. A., Donahue, N., Kjaergaard, H. G., and Ehn, M.: Highly Oxygenated Organic Molecules (HOM) from Gas-Phase Autoxidation Involving Peroxy Radicals: A Key Contributor to Atmospheric Aerosol, *Chem. Rev.*, 119, 3472-3509, 10.1021/acs.chemrev.8b00395, 2019.
- Boyd, C. M., Sanchez, J., Xu, L., Eugene, A. J., Nah, T., Tuet, W. Y., Guzman, M. I., and Ng, N. L.: Secondary organic aerosol formation from the beta-pinene+ NO_3 system: effect of humidity and peroxy radical fate, *Atmos. Chem. Phys.*, 15, 7497-7522, 10.5194/acp-15-7497-2015, 2015.
- Boyd, C. M., Nah, T., Xu, L., Berkemeier, T., and Ng, N. L.: Secondary Organic Aerosol (SOA) from Nitrate Radical Oxidation of Monoterpenes: Effects of Temperature, Dilution, and Humidity on Aerosol Formation, Mixing, and Evaporation, *Environ. Sci. Technol.*, 51, 7831-7841, 10.1021/acs.est.7b01460, 2017.
- Brown, S. S., deGouw, J. A., Warneke, C., Ryerson, T. B., Dube, W. P., Atlas, E., Weber, R. J., Peltier, R. E., Neuman, J. A., Roberts, J. M., Swanson, A., Flocke, F., McKeen, S. A., Brioude, J., Sommariva, R., Trainer, M., Fehsenfeld, F. C., and Ravishankara, A. R.: Nocturnal isoprene oxidation over the Northeast United States in summer and its impact on reactive nitrogen partitioning and secondary organic aerosol, *Atmos. Chem. Phys.*, 9, 3027-3042, 10.5194/acp-9-3027-2009, 2009.
- Brown, S. S., Dube, W. P., Peischl, J., Ryerson, T. B., Atlas, E., Warneke, C., de Gouw, J. A., Hekkert, S. t. L., Brock, C. A., Flocke, F., Trainer, M., Parrish, D. D., Fehsenfeld, F. C., and Ravishankara, A. R.: Budgets for nocturnal VOC oxidation by nitrate radicals aloft during the 2006 Texas Air Quality Study, *J. Geophys. Res.-Atmos.*, 116, 10.1029/2011jd016544, 2011.
- Brown, S. S., and Stutz, J.: Nighttime radical observations and chemistry, *Chem. Soc. Rev.*, 41, 6405-6447, 10.1039/c2cs35181a, 2012.

- Chen, J., Møller, K. H., Wennberg, P. O., and Kjaergaard, H. G.: Unimolecular Reactions Following Indoor and Outdoor Limonene Ozonolysis, *J. Phys. Chem. A* 125, 669-680, 10.1021/acs.jpca.0c09882, 2021.
- Chen, Y. L., Takeuchi, M., Nah, T., Xu, L., Canagaratna, M. R., Stark, H., Baumann, K., Canonaco, F., Prevot, A. S. H., Huey, L. G., Weber, R. J., and Ng, N. L.: Chemical characterization of secondary organic aerosol at a rural site in the southeastern US: insights from simultaneous high-resolution time-of-flight aerosol mass spectrometer (HR-ToF-AMS) and FIGAERO chemical ionization mass spectrometer (CIMS) measurements, *Atmos. Chem. Phys.*, 20, 8421-8440, 10.5194/acp-20-8421-2020, 2020.
- Clafin, M. S., and Ziemann, P. J.: Identification and Quantitation of Aerosol Products of the Reaction of β -Pinene with NO_3 Radicals and Implications for Gas- and Particle-Phase Reaction Mechanisms, *The Journal of Physical Chemistry A*, 122, 3640-3652, 10.1021/acs.jpca.8b00692, 2018.
- Crouse, J. D., Knap, H. C., Ørnsø, K. B., Jørgensen, S., Paulot, F., Kjaergaard, H. G., and Wennberg, P. O.: Atmospheric Fate of Methacrolein. 1. Peroxy Radical Isomerization Following Addition of OH and O_2 , *The Journal of Physical Chemistry A*, 116, 5756-5762, 10.1021/jp211560u, 2012.
- Crouse, J. D., Nielsen, L. B., Jørgensen, S., Kjaergaard, H. G., and Wennberg, P. O.: Autoxidation of Organic Compounds in the Atmosphere, *J. Phys. Chem. Lett.* , 4, 3513-3520, 10.1021/jz4019207, 2013.
- Draper, D. C., Myllys, N., Hyttinen, N., Møller, K. H., Kjaergaard, H. G., Fry, J. L., Smith, J. N., and Kurten, T.: Formation of Highly Oxidized Molecules from NO_3 Radical Initiated Oxidation of Delta-3-Carene: A Mechanistic Study, *Acs Earth and Space Chemistry*, 3, 1460-1470, 10.1021/acsearthspacechem.9b00143, 2019.
- Ehn, M., Thornton, J. A., Kleist, E., Sipila, M., Junninen, H., Pullinen, I., Springer, M., Rubach, F., Tillmann, R., Lee, B., Lopez-Hilfiker, F., Andres, S., Acir, I. H., Rissanen, M., Jokinen, T., Schobesberger, S., Kangasluoma, J., Kontkanen, J., Nieminen, T., Kurten, T., Nielsen, L. B., Jørgensen, S., Kjaergaard, H. G., Canagaratna, M., Dal Maso, M., Berndt, T., Petaja, T., Wahner, A., Kerminen, V. M., Kulmala, M., Worsnop, D. R., Wildt, J., and Mentel, T. F.: A large source of low-volatility secondary organic aerosol, *Nature*, 506, 476-479, 10.1038/nature13032, 2014.
- Ehn, M., Berndt, T., Wildt, J., and Mentel, T.: Highly Oxygenated Molecules from Atmospheric Autoxidation of Hydrocarbons: A Prominent Challenge for Chemical Kinetics Studies, *Int. J. Chem. Kinet.* , 49, 821-831, 10.1002/kin.21130, 2017.
- Eisele, F. L., and Tanner, D. J.: Measurement of the gas phase concentration of H_2SO_4 and methane sulfonic acid and estimates of H_2SO_4 production and loss in the atmosphere, 98, 9001-9010, 10.1029/93jd00031, 1993.
- Faxon, C., Hammes, J., Le Breton, M., Pathak, R. K., and Hallquist, M.: Characterization of organic nitrate constituents of secondary organic aerosol (SOA) from nitrate-radical-initiated oxidation of limonene using high-resolution chemical ionization mass spectrometry, *Atmos. Chem. Phys.*, 18, 5467-5481, 10.5194/acp-18-5467-2018, 2018.
- Finlayson-Pitts, B., and Pitts, J.: *Chemistry of the upper and lower atmosphere*, Academic Press, San Diego, 2000.
- Fry, J. L., Kiendler-Scharr, A., Rollins, A. W., Wooldridge, P. J., Brown, S. S., Fuchs, H., Dube, W., Mensah, A., dal Maso, M., Tillmann, R., Dorn, H. P., Brauers, T., and Cohen, R. C.: Organic nitrate and secondary organic aerosol yield from NO_3 oxidation of beta-pinene evaluated using a gas-phase kinetics/aerosol partitioning model, *Atmos. Chem. Phys.*, 9, 1431-1449, 2009.
- Fry, J. L., Kiendler-Scharr, A., Rollins, A. W., Brauers, T., Brown, S. S., Dorn, H. P., Dube, W. P., Fuchs, H., Mensah, A., Rohrer, F., Tillmann, R., Wahner, A., Wooldridge, P. J., and Cohen, R. C.: SOA from limonene: role of NO_3 in its generation and degradation, *Atmos. Chem. Phys.*, 11, 3879-3894, 10.5194/acp-11-3879-2011, 2011.
- Fry, J. L., Draper, D. C., Barsanti, K. C., Smith, J. N., Ortega, J., Winkle, P. M., Lawler, M. J., Brown, S. S., Edwards, P. M., Cohen, R. C., and Lee, L.: Secondary Organic Aerosol Formation and Organic Nitrate Yield from NO_3 Oxidation of Biogenic Hydrocarbons, *Environ. Sci. Technol.*, 48, 11944-11953, 10.1021/es502204x, 2014.

Fry, J. L., Brown, S. S., Middlebrook, A. M., Edwards, P. M., Campuzano-Jost, P., Day, D. A., Jimenez, J. L., Allen, H. M., Ryerson, T. B., Pollack, I., Graus, M., Warneke, C., de Gouw, J. A., Brock, C. A., Gilman, J., Lerner, B. M., Dube, W. P., Liao, J., and Welti, A.: Secondary organic aerosol (SOA) yields from NO₃ radical + isoprene based on nighttime aircraft power plant plume transects, *Atmos. Chem. Phys.*, 18, 11663-11682, 10.5194/acp-18-11663-2018, 2018.

Fuchs, H., Dorn, H. P., Bachner, M., Bohn, B., Brauers, T., Gomm, S., Hofzumahaus, A., Holland, F., Nehr, S., Rohrer, F., Tillmann, R., and Wahner, A.: Comparison of OH concentration measurements by DOAS and LIF during SAPHIR chamber experiments at high OH reactivity and low NO concentration, *Atmos. Meas. Tech.*, 5, 1611-1626, 10.5194/amt-5-1611-2012, 2012.

Garmash, O., Rissanen, M. P., Pullinen, I., Schmitt, S., Kausiala, O., Tillmann, R., Percival, C., Bannan, T. J., Priestley, M., Hallquist, Å. M., Kleist, E., Kiendler-Scharr, A., Hallquist, M., Berndt, T., McFiggans, G., Wildt, J., Mentel, T., and Ehn, M.: Multi-generation OH oxidation as a source for highly oxygenated organic molecules from aromatics, *Atmos. Chem. Phys. Discuss.*, 2019, 1-33, 10.5194/acp-2019-582, 2019.

Geyer, A., Alicke, B., Konrad, S., Schmitz, T., Stutz, J., and Platt, U.: Chemistry and oxidation capacity of the nitrate radical in the continental boundary layer near Berlin, *J. Geophys. Res.-Atmos.*, 106, 8013-8025, 10.1029/2000jd900681, 2001.

Hamilton, J. F., Bryant, D. J., Edwards, P. M., Ouyang, B., Bannan, T. J., Mehra, A., Mayhew, A. W., Hopkins, J. R., Dunmore, R. E., Squires, F. A., Lee, J. D., Newland, M. J., Worrall, S. D., Bacak, A., Coe, H., Percival, C., Whalley, L. K., Heard, D. E., Slater, E. J., Jones, R. L., Cui, T., Surratt, J. D., Reeves, C. E., Mills, G. P., Grimmond, S., Sun, Y., Xu, W., Shi, Z., and Rickard, A. R.: Key Role of NO₃ Radicals in the Production of Isoprene Nitrates and Nitrooxyorganosulfates in Beijing, *Environ. Sci. Technol.*, 55, 842-853, 10.1021/acs.est.0c05689, 2021.

Huang, W., Saathoff, H., Shen, X. L., Ramisetty, R., Leisner, T., and Mohr, C.: Chemical Characterization of Highly Functionalized Organonitrates Contributing to Night-Time Organic Aerosol Mass Loadings and Particle Growth, *Environ. Sci. Technol.*, 53, 1165-1174, 10.1021/acs.est.8b05826, 2019.

Hyttinen, N., Kupiainen-Määttä, O., Rissanen, M. P., Muuronen, M., Ehn, M., and Kurtén, T.: Modeling the Charging of Highly Oxidized Cyclohexene Ozonolysis Products Using Nitrate-Based Chemical Ionization, *The Journal of Physical Chemistry A*, 119, 6339-6345, 10.1021/acs.jpca.5b01818, 2015.

Japar, S. M., and Niki, H.: Gas-phase reactions of the nitrate radical with olefins, *The Journal of Physical Chemistry*, 79, 1629-1632, 10.1021/j100583a002, 1975.

Jenkin, M. E., Saunders, S. M., and Pilling, M. J.: The tropospheric degradation of volatile organic compounds: A protocol for mechanism development, *Atmos. Environ.*, 31, 81-104, 10.1016/s1352-2310(96)00105-7, 1997.

Jenkin, M. E., Boyd, A. A., and Lesclaux, R.: Peroxy Radical Kinetics Resulting from the OH-Initiated Oxidation of 1,3-Butadiene, 2,3-Dimethyl-1,3-Butadiene and Isoprene, *J. Atmos. Chem.*, 29, 267-298, 10.1023/A:1005940332441, 1998.

Jenkin, M. E., Saunders, S. M., Wagner, V., and Pilling, M. J.: Protocol for the development of the Master Chemical Mechanism, MCM v3 (Part B): tropospheric degradation of aromatic volatile organic compounds, *Atmos. Chem. Phys.*, 3, 181-193, 2003.

Jenkin, M. E., Young, J. C., and Rickard, A. R.: The MCM v3.3.1 degradation scheme for isoprene, *Atmos. Chem. Phys.*, 15, 11433-11459, 10.5194/acp-15-11433-2015, 2015.

Jokinen, T., Sipila, M., Junninen, H., Ehn, M., Lonn, G., Hakala, J., Petaja, T., Mauldin, R. L., III, Kulmala, M., and Worsnop, D. R.: Atmospheric sulphuric acid and neutral cluster measurements using CI-API-TOF, *Atmos. Chem. Phys.*, 12, 4117-4125, 10.5194/acp-12-4117-2012, 2012.

- Jokinen, T., Sipila, M., Richters, S., Kerminen, V. M., Paasonen, P., Stratmann, F., Worsnop, D., Kulmala, M., Ehn, M., Herrmann, H., and Berndt, T.: Rapid Autoxidation Forms Highly Oxidized RO₂ Radicals in the Atmosphere, *Angew. Chem.-Int. Edit.*, 53, 14596-14600, 10.1002/anie.201408566, 2014.
- Jokinen, T., Berndt, T., Makkonen, R., Kerminen, V. M., Junninen, H., Paasonen, P., Stratmann, F., Herrmann, H., Guenther, A. B., Worsnop, D. R., Kulmala, M., Ehn, M., and Sipila, M.: Production of extremely low volatile organic compounds from biogenic emissions: Measured yields and atmospheric implications, *Proc. Nat. Acad. Sci. U.S.A.*, 112, 7123-7128, 10.1073/pnas.1423977112, 2015.
- Kaminski, M., Fuchs, H., Acir, I.-H., Bohn, B., Brauers, T., Dorn, H.-P., Haeseler, R., Hofzumahaus, A., Li, X., Lutz, A., Nehr, S., Rohrer, F., Tillmann, R., Vereecken, L., Wegener, R., and Wahner, A.: Investigation of the beta-pinene photooxidation by OH in the atmosphere simulation chamber SAPHIR, *Atmos. Chem. Phys.*, 17, 6631-6650, 10.5194/acp-17-6631-2017, 2017.
- Kenseth, C. M., Huang, Y. L., Zhao, R., Dalleska, N. F., Hethcox, C., Stoltz, B. M., and Seinfeld, J. H.: Synergistic O₃ + OH oxidation pathway to extremely low-volatility dimers revealed in beta-pinene secondary organic aerosol, *Proc. Nat. Acad. Sci. U.S.A.*, 115, 8301-8306, 10.1073/pnas.1804671115, 2018.
- Kirkby, J., Duplissy, J., Sengupta, K., Frege, C., Gordon, H., Williamson, C., Heinritzi, M., Simon, M., Yan, C., Almeida, J., Tröstl, J., Nieminen, T., Ortega, I. K., Wagner, R., Adamov, A., Amorim, A., Bernhammer, A.-K., Bianchi, F., Breitenlechner, M., Brilke, S., Chen, X., Craven, J., Dias, A., Ehrhart, S., Flagan, R. C., Franchin, A., Fuchs, C., Guida, R., Hakala, J., Hoyle, C. R., Jokinen, T., Junninen, H., Kangasluoma, J., Kim, J., Krapf, M., Kürten, A., Laaksonen, A., Lehtipalo, K., Makhmutov, V., Mathot, S., Molteni, U., Onnela, A., Peräkylä, O., Piel, F., Petäjä, T., Praplan, A. P., Pringle, K., Rap, A., Richards, N. A. D., Riipinen, I., Rissanen, M. P., Rondo, L., Sarnela, N., Schobesberger, S., Scott, C. E., Seinfeld, J. H., Sipilä, M., Steiner, G., Stozhkov, Y., Stratmann, F., Tomé, A., Virtanen, A., Vogel, A. L., Wagner, A. C., Wagner, P. E., Weingartner, E., Wimmer, D., Winkler, P. M., Ye, P., Zhang, X., Hansel, A., Dommen, J., Donahue, N. M., Worsnop, D. R., Baltensperger, U., Kulmala, M., Carslaw, K. S., and Curtius, J.: Ion-induced nucleation of pure biogenic particles, *Nature*, 533, 521-526, 10.1038/nature17953, 2016.
- Krechmer, J. E., Coggon, M. M., Massoli, P., Nguyen, T. B., Crouse, J. D., Hu, W. W., Day, D. A., Tyndall, G. S., Henze, D. K., Rivera-Rios, J. C., Nowak, J. B., Kimmel, J. R., Mauldin, R. L., Stark, H., Jayne, J. T., Sipila, M., Junninen, H., St Clair, J. M., Zhang, X., Feiner, P. A., Zhang, L., Miller, D. O., Brune, W. H., Keutsch, F. N., Wennberg, P. O., Seinfeld, J. H., Worsnop, D. R., Jimenez, J. L., and Canagaratna, M. R.: Formation of Low Volatility Organic Compounds and Secondary Organic Aerosol from Isoprene Hydroxyhydroperoxide Low-NO Oxidation, *Environ. Sci. Technol.*, 49, 10330-10339, 10.1021/acs.est.5b02031, 2015.
- Kwan, A. J., Chan, A. W. H., Ng, N. L., Kjaergaard, H. G., Seinfeld, J. H., and Wennberg, P. O.: Peroxy radical chemistry and OH radical production during the NO₃-initiated oxidation of isoprene, *Atmos. Chem. Phys.*, 12, 7499-7515, 10.5194/acp-12-7499-2012, 2012.
- Lai, C. C., and Finlayson-Pitts, B. J.: Reactions of dinitrogen pentoxide and nitrogen-dioxide with 1-palmitoyl-2-oleoyl-sn-glycero-3-phosphocholine, *Lipids*, 26, 306-314, 10.1007/bf02537142, 1991.
- Lee, B. H., Mohr, C., Lopez-Hilfiker, F. D., Lutz, A., Hallquist, M., Lee, L., Romer, P., Cohen, R. C., Iyer, S., Kurten, T., Hu, W., Day, D. A., Campuzano-Jost, P., Jimenez, J. L., Xu, L., Ng, N. L., Guo, H., Weber, R. J., Wild, R. J., Brown, S. S., Koss, A., de Gouw, J., Olson, K., Goldstein, A. H., Seco, R., Kim, S., McAvey, K., Shepson, P. B., Starn, T., Baumann, K., Edgerton, E. S., Liu, J., Shilling, J. E., Miller, D. O., Brune, W., Schobesberger, S., D'Ambro, E. L., and Thornton, J. A.: Highly functionalized organic nitrates in the southeast United States: Contribution to secondary organic aerosol and reactive nitrogen budgets, *Proc. Nat. Acad. Sci. U.S.A.*, 113, 1516-1521, 10.1073/pnas.1508108113, 2016.
- Lu, K. D., Rohrer, F., Holland, F., Fuchs, H., Brauers, T., Oebel, A., Dlugi, R., Hu, M., Li, X., Lou, S. R., Shao, M., Zhu, T., Wahner, A., Zhang, Y. H., and Hofzumahaus, A.: Nighttime observation and chemistry of HO_x in the Pearl River Delta and Beijing in summer 2006, *Atmos. Chem. Phys.*, 14, 4979-4999, 10.5194/acp-14-4979-2014, 2014.

- Malkin, T. L., Goddard, A., Heard, D. E., and Seakins, P. W.: Measurements of OH and HO₂ yields from the gas phase ozonolysis of isoprene, *Atmos. Chem. Phys.*, 10, 1441-1459, 10.5194/acp-10-1441-2010, 2010.
- Massoli, P., Stark, H., Canagaratna, M. R., Krechmer, J. E., Xu, L., Ng, N. L., Mauldin, R. L., Yan, C., Kimmel, J., Misztal, P. K., Jimenez, J. L., Jayne, J. T., and Worsnop, D. R.: Ambient Measurements of Highly Oxidized Gas-Phase Molecules during the Southern Oxidant and Aerosol Study (SOAS) 2013, *ACS Earth and Space Chemistry*, 2, 653-672, 10.1021/acsearthspacechem.8b00028, 2018.
- McFiggans, G., Mentel, T. F., Wildt, J., Pullinen, I., Kang, S., Kleist, E., Schmitt, S., Springer, M., Tillmann, R., Wu, C., Zhao, D., Hallquist, M., Faxon, C., Le Breton, M., Hallquist, Å. M., Simpson, D., Bergström, R., Jenkin, M. E., Ehn, M., Thornton, J. A., Alfarra, M. R., Bannan, T. J., Percival, C. J., Priestley, M., Topping, D., and Kiendler-Scharr, A.: Secondary organic aerosol reduced by mixture of atmospheric vapours, *Nature*, 565, 587-593, 10.1038/s41586-018-0871-y, 2019.
- Mentel, T. F., Springer, M., Ehn, M., Kleist, E., Pullinen, I., Kurten, T., Rissanen, M., Wahner, A., and Wildt, J.: Formation of highly oxidized multifunctional compounds: autoxidation of peroxy radicals formed in the ozonolysis of alkenes - deduced from structure-product relationships, *Atmos. Chem. Phys.*, 15, 6745-6765, 10.5194/acp-15-6745-2015, 2015.
- Møller, K. H., Bates, K. H., and Kjaergaard, H. G.: The Importance of Peroxy Radical Hydrogen-Shift Reactions in Atmospheric Isoprene Oxidation, *J. Phys. Chem. A* 123, 920-932, 10.1021/acs.jpca.8b10432, 2019.
- Molteni, U., Bianchi, F., Klein, F., El Haddad, I., Frege, C., Rossi, M. J., Dommen, J., and Baltensperger, U.: Formation of highly oxygenated organic molecules from aromatic compounds, *Atmos. Chem. Phys.*, 18, 1909-1921, 10.5194/acp-18-1909-2018, 2018.
- Molteni, U., Simon, M., Heinritzi, M., Hoyle, C. R., Bernhammer, A. K., Bianchi, F., Breitenlechner, M., Brilke, S., Dias, A., Duplissy, J., Frege, C., Gordon, H., Heyn, C., Jokinen, T., Kurten, A., Lehtipalo, K., Makhmutov, V., Petaja, T., Pieber, S. M., Praplan, A. P., Schobesberger, S., Steiner, G., Stozhkov, Y., Tome, A., Trostl, J., Wagner, A. C., Wagner, R., Williamson, C., Yan, C., Baltensperger, U., Curtius, J., Donahue, N. M., Hansel, A., Kirkby, J., Kulmala, M., Worsnop, D. R., and Dommen, J.: Formation of Highly Oxygenated Organic Molecules from alpha-Pinene Ozonolysis: Chemical Characteristics, Mechanism, and Kinetic Model Development, *Acs Earth and Space Chemistry*, 3, 873-883, 10.1021/acsearthspacechem.9b00035, 2019.
- Nah, T., Sanchez, J., Boyd, C. M., and Ng, N. L.: Photochemical Aging of alpha-pinene and beta-pinene Secondary Organic Aerosol formed from Nitrate Radical Oxidation, *Environ. Sci. Technol.*, 50, 222-231, 10.1021/acs.est.5b04594, 2016.
- Ng, N. L., Kwan, A. J., Surratt, J. D., Chan, A. W. H., Chhabra, P. S., Sorooshian, A., Pye, H. O. T., Crounse, J. D., Wennberg, P. O., Flagan, R. C., and Seinfeld, J. H.: Secondary organic aerosol (SOA) formation from reaction of isoprene with nitrate radicals (NO₃), *Atmos. Chem. Phys.*, 8, 4117-4140, 10.5194/acp-8-4117-2008, 2008.
- Nguyen, T. B., Tyndall, G. S., Crounse, J. D., Teng, A. P., Bates, K. H., Schwantes, R. H., Coggon, M. M., Zhang, L., Feiner, P., Milller, D. O., Skog, K. M., Rivera-Rios, J. C., Dorris, M., Olson, K. F., Koss, A., Wild, R. J., Brown, S. S., Goldstein, A. H., de Gouw, J. A., Brune, W. H., Keutsch, F. N., Seinfeld, J. H., and Wennberg, P. O.: Atmospheric fates of Criegee intermediates in the ozonolysis of isoprene, *Phys. Chem. Chem. Phys.*, 18, 10241-10254, 10.1039/c6cp00053c, 2016.
- Novelli, A., Cho, C., Fuchs, H., Hofzumahaus, A., Rohrer, F., Tillmann, R., Kiendler-Scharr, A., Wahner, A., and Vereecken, L.: Experimental and theoretical study on the impact of a nitrate group on the chemistry of alkoxy radicals, *Phys. Chem. Chem. Phys.*, 23, 5474-5495, 10.1039/D0CP05555G, 2021.
- Nozière, B., and Vereecken, L.: Direct Observation of Aliphatic Peroxy Radical Autoxidation and Water Effects: An Experimental and Theoretical Study, *Angew. Chem.-Int. Edit.*, 58, 13976-13982, 10.1002/anie.201907981, 2019.

- Perring, A. E., Wisthaler, A., Graus, M., Wooldridge, P. J., Lockwood, A. L., Mielke, L. H., Shepson, P. B., Hansel, A., and Cohen, R. C.: A product study of the isoprene+NO₃ reaction, *Atmos. Chem. Phys.*, 9, 4945-4956, 10.5194/acp-9-4945-2009, 2009.
- Pfrang, C., Martin, R. S., Canosa-Mas, C. E., and Wayne, R. P.: Gas-phase reactions of NO₃ and N₂O₅ with (Z)-hex-4-en-1-ol, (Z)-hex-3-en-1-ol ('leaf alcohol'), (E)-hex-3-en-1-ol, (Z)-hex-2-en-1-ol and (E)-hex-2-en-1-ol, *Phys. Chem. Chem. Phys.*, 8, 354-363, 10.1039/b510835g, 2006.
- Pullinen, I., Schmitt, S., Kang, S., Sarrafzadeh, M., Schlag, P., Andres, S., Kleist, E., Mentel, T. F., Rohrer, F., Springer, M., Tillmann, R., Wildt, J., Wu, C., Zhao, D., Wahner, A., and Kiendler-Scharr, A.: Impact of NO_x on secondary organic aerosol (SOA) formation from α -pinene and β -pinene photooxidation: the role of highly oxygenated organic nitrates, *Atmos. Chem. Phys.*, 20, 10125-10147, 10.5194/acp-20-10125-2020, 2020.
- Quelever, L. L. J., Kristensen, K., Jensen, L. N., Rosati, B., Teiwes, R., Daellenbach, K. R., Perakyla, O., Roldin, P., Bossi, R., Pedersen, H. B., Glasius, M., Bilde, M., and Ehn, M.: Effect of temperature on the formation of highly oxygenated organic molecules (HOMs) from alpha-pinene ozonolysis, *Atmos. Chem. Phys.*, 19, 7609-7625, 10.5194/acp-19-7609-2019, 2019.
- Richters, S., Pfeifle, M., Olzmann, M., and Berndt, T.: endo-Cyclization of unsaturated RO₂ radicals from the gas-phase ozonolysis of cyclohexadienes, *Chem. Commun.*, 53, 4132-4135, 10.1039/c7cc01350g, 2017.
- Rissanen, M. P., Kurten, T., Sipila, M., Thornton, J. A., Kangasluoma, J., Sarnela, N., Junninen, H., Jørgensen, S., Schallhart, S., Kajos, M. K., Taipale, R., Springer, M., Mentel, T. F., Ruuskanen, T., Petaja, T., Worsnop, D. R., Kjaergaard, H. G., and Ehn, M.: The Formation of Highly Oxidized Multifunctional Products in the Ozonolysis of Cyclohexene, *J. Am. Chem. Soc.*, 136, 15596-15606, 10.1021/ja507146s, 2014.
- Rissanen, M. P., Kurten, T., Sipila, M., Thornton, J. A., Kausiala, O., Garmash, O., Kjaergaard, H. G., Petaja, T., Worsnop, D. R., Ehn, M., and Kulmala, M.: Effects of Chemical Complexity on the Autoxidation Mechanisms of Endocyclic Alkene Ozonolysis Products: From Methylcyclohexenes toward Understanding alpha-Pinene, *J. Phys. Chem. A* 119, 4633-4650, 10.1021/jp510966g, 2015.
- Riva, M., Rantala, P., Krechmer, J. E., Perakyla, O., Zhang, Y. J., Heikkinen, L., Garmash, O., Yan, C., Kulmala, M., Worsnop, D., and Ehn, M.: Evaluating the performance of five different chemical ionization techniques for detecting gaseous oxygenated organic species, *Atmos. Meas. Tech.*, 12, 2403-2421, 10.5194/amt-12-2403-2019, 2019.
- Rohrer, F., Bohn, B., Brauers, T., Bruning, D., Johnen, F. J., Wahner, A., and Kleffmann, J.: Characterisation of the photolytic HONO-source in the atmosphere simulation chamber SAPHIR, *Atmos. Chem. Phys.*, 5, 2189-2201, 2005.
- Rollins, A. W., Kiendler-Scharr, A., Fry, J. L., Brauers, T., Brown, S. S., Dorn, H. P., Dube, W. P., Fuchs, H., Mensah, A., Mentel, T. F., Rohrer, F., Tillmann, R., Wegener, R., Wooldridge, P. J., and Cohen, R. C.: Isoprene oxidation by nitrate radical: alkyl nitrate and secondary organic aerosol yields, *Atmos. Chem. Phys.*, 9, 6685-6703, 2009.
- Saunders, S. M., Jenkin, M. E., Derwent, R. G., and Pilling, M. J.: Protocol for the development of the Master Chemical Mechanism, MCM v3 (Part A): tropospheric degradation of non-aromatic volatile organic compounds, *Atmos. Chem. Phys.*, 3, 161-180, 2003.
- Schwantes, R. H., Teng, A. P., Nguyen, T. B., Coggon, M. M., Crouse, J. D., St Clair, J. M., Zhang, X., Schilling, K. A., Seinfeld, J. H., and Wennberg, P. O.: Isoprene NO₃ Oxidation Products from the RO₂ + HO₂ Pathway, *J. Phys. Chem. A* 119, 10158-10171, 10.1021/acs.jpca.5b06355, 2015.
- Skov, H., Hjorth, J., Lohse, C., Jensen, N. R., and Restelli, G.: Products and mechanisms of the reactions of the nitrate radical (NO₃) with isoprene, 1,3-butadiene and 2,3-dimethyl-1,3-butadiene in air, *Atmospheric Environment. Part A. General Topics*, 26, 2771-2783, [https://doi.org/10.1016/0960-1686\(92\)90015-D](https://doi.org/10.1016/0960-1686(92)90015-D), 1992.
- Stark, M. S.: Epoxidation of Alkenes by Peroxyl Radicals in the Gas Phase: Structure–Activity Relationships, *The Journal of Physical Chemistry A*, 101, 8296-8301, 10.1021/jp972054+, 1997.

- Stark, M. S.: Addition of Peroxyl Radicals to Alkenes and the Reaction of Oxygen with Alkyl Radicals, *J. Am. Chem. Soc.*, 122, 4162-4170, 10.1021/ja993760m, 2000.
- Starn, T. K., Shepson, P. B., Bertman, S. B., Riemer, D. D., Zika, R. G., and Olszyna, K.: Nighttime isoprene chemistry at an urban-impacted forest site, 103, 22437-22447, <https://doi.org/10.1029/98JD01201>, 1998.
- Stroud, C. A., Roberts, J. M., Williams, E. J., Hereid, D., Angevine, W. M., Fehsenfeld, F. C., Wisthaler, A., Hansel, A., Martinez-Harder, M., Harder, H., Brune, W. H., Hoenninger, G., Stutz, J., and White, A. B.: Nighttime isoprene trends at an urban forested site during the 1999 Southern Oxidant Study, 107, ACH 7-1-ACH 7-14, <https://doi.org/10.1029/2001JD000959>, 2002.
- Takeuchi, M., and Ng, N. L.: Chemical composition and hydrolysis of organic nitrate aerosol formed from hydroxyl and nitrate radical oxidation of alpha-pinene and beta-pinene, *Atmos. Chem. Phys.*, 19, 12749-12766, 10.5194/acp-19-12749-2019, 2019.
- Tan, Z. F., Lu, K. D., Hofzumahaus, A., Fuchs, H., Bohn, B., Holland, F., Liu, Y. H., Rohrer, F., Shao, M., Sun, K., Wu, Y. S., Zeng, L. M., Zhang, Y. S., Zou, Q., Kiendler-Scharr, A., Wahner, A., and Zhang, Y. H.: Experimental budgets of OH, HO₂, and RO₂ radicals and implications for ozone formation in the Pearl River Delta in China 2014, *Atmos. Chem. Phys.*, 19, 7129-7150, 10.5194/acp-19-7129-2019, 2019.
- Tröstl, J., Chuang, W. K., Gordon, H., Heinritzi, M., Yan, C., Molteni, U., Ahlm, L., Frege, C., Bianchi, F., Wagner, R., Simon, M., Lehtipalo, K., Williamson, C., Craven, J. S., Duplissy, J., Adamov, A., Almeida, J., Bernhammer, A.-K., Breitenlechner, M., Brilke, S., Dias, A., Ehrhart, S., Flagan, R. C., Franchin, A., Fuchs, C., Guida, R., Gysel, M., Hansel, A., Hoyle, C. R., Jokinen, T., Junninen, H., Kangasluoma, J., Keskinen, H., Kim, J., Krapf, M., Kürten, A., Laaksonen, A., Lawler, M., Leiminger, M., Mathot, S., Möhler, O., Nieminen, T., Onnela, A., Petäjä, T., Piel, F. M., Miettinen, P., Rissanen, M. P., Rondo, L., Sarnela, N., Schobesberger, S., Sengupta, K., Sipilä, M., Smith, J. N., Steiner, G., Tomè, A., Virtanen, A., Wagner, A. C., Weingartner, E., Wimmer, D., Winkler, P. M., Ye, P., Carslaw, K. S., Curtius, J., Dommen, J., Kirkby, J., Kulmala, M., Riipinen, I., Worsnop, D. R., Donahue, N. M., and Baltensperger, U.: The role of low-volatility organic compounds in initial particle growth in the atmosphere, *Nature*, 533, 527-531, 10.1038/nature18271, 2016.
- Valiev, R. R., Hasan, G., Salo, V.-T., Kubecka, J., and Kurten, T.: Intersystem Crossings Drive Atmospheric Gas-Phase Dimer Formation, *The journal of physical chemistry. A*, 123, 6596-6604, 10.1021/acs.jpca.9b02559, 2019.
- Vereecken, L., and Peeters, J.: Nontraditional (per)oxy ring-closure paths in the atmospheric oxidation of isoprene and monoterpenes, *J. Phys. Chem. A* 108, 5197-5204, 10.1021/jp049219g, 2004.
- Vereecken, L., Mueller, J. F., and Peeters, J.: Low-volatility poly-oxygenates in the OH-initiated atmospheric oxidation of alpha-pinene: impact of non-traditional peroxy radical chemistry, *Phys. Chem. Chem. Phys.*, 9, 5241-5248, 10.1039/b708023a, 2007.
- Vereecken, L., and Peeters, J.: A structure-activity relationship for the rate coefficient of H-migration in substituted alkoxy radicals, *Phys. Chem. Chem. Phys.*, 12, 12608-12620, 10.1039/c0cp00387e, 2010.
- Vereecken, L., and Francisco, J. S.: Theoretical studies of atmospheric reaction mechanisms in the troposphere, *Chem. Soc. Rev.*, 41, 6259-6293, 10.1039/c2cs35070j, 2012.
- Vereecken, L., and Peeters, J.: A theoretical study of the OH-initiated gas-phase oxidation mechanism of beta-pinene (C₁₀H₁₆): first generation products, *Phys. Chem. Chem. Phys.*, 14, 3802-3815, 10.1039/c2cp23711c, 2012.
- Vereecken, L., and Nozière, B.: H migration in peroxy radicals under atmospheric conditions, *Atmos. Chem. Phys.*, 20, 7429-7458, 10.5194/acp-20-7429-2020, 2020.
- Vereecken, L., Carlsson, P. T. M., Novelli, A., Bernard, F., Brown, S. S., Cho, C., Crowley, J. N., Fuchs, H., Mellouki, W., Reimer, D., Shenolikar, J., Tillmann, R., Zhou, L., Kiendler-Scharr, A., and Wahner, A.: Theoretical and experimental study of peroxy and alkoxy radicals in the NO₃-initiated oxidation of isoprene, *Phys. Chem. Chem. Phys.*, 23, 5496-5515, 10.1039/d0cp06267g, 2021.

Viggiano, A. A., Seeley, J. V., Mundis, P. L., Williamson, J. S., and Morris, R. A.: Rate Constants for the Reactions of $\text{XO}_3\text{-(H}_2\text{O)}_n$ ($\text{X} = \text{C, HC, and N}$) and $\text{NO}_3\text{-(HNO}_3)_n$ with H_2SO_4 : Implications for Atmospheric Detection of H_2SO_4 , *The Journal of Physical Chemistry A*, 101, 8275-8278, 10.1021/jp971768h, 1997.

Wagner, N. L., Dubé, W. P., Washenfelder, R. A., Young, C. J., Pollack, I. B., Ryerson, T. B., and Brown, S. S.: Diode laser-based cavity ring-down instrument for NO_3 , N_2O_5 , NO , NO_2 and O_3 from aircraft, *Atmos. Meas. Tech.*, 4, 1227-1240, 10.5194/amt-4-1227-2011, 2011.

Wang, Y., Mehra, A., Krechmer, J. E., Yang, G., Hu, X., Lu, Y., Lambe, A., Canagaratna, M., Chen, J., Worsnop, D., Coe, H., and Wang, L.: Oxygenated products formed from OH-initiated reactions of trimethylbenzene: autoxidation and accretion, *Atmos. Chem. Phys.*, 20, 9563-9579, 10.5194/acp-20-9563-2020, 2020.

Wennberg, P. O., Bates, K. H., Crounse, J. D., Dodson, L. G., McVay, R. C., Mertens, L. A., Nguyen, T. B., Praske, E., Schwantes, R. H., Smarte, M. D., St Clair, J. M., Teng, A. P., Zhang, X., and Seinfeld, J. H.: Gas-Phase Reactions of Isoprene and Its Major Oxidation Products, *Chem. Rev.*, 118, 3337-3390, 10.1021/acs.chemrev.7b00439, 2018.

Wu, R., Vereecken, L., Tsiligiannis, E., Kang, S., Albrecht, S. R., Hantschke, L., Zhao, D., Novelli, A., Fuchs, H., Tillmann, R., Hohaus, T., Carlsson, P. T. M., Shenolikar, J., Bernard, F., Crowley, J. N., Fry, J. L., Brownwood, B., Thornton, J. A., Brown, S. S., Kiendler-Scharr, A., Wahner, A., Hallquist, M., and Mentel, T. F.: Molecular composition and volatility of multi-generation products formed from isoprene oxidation by nitrate radical, *Atmos. Chem. Phys. Discuss.*, 2020, 1-37, 10.5194/acp-2020-1180, 2020.

Xu, L., Guo, H. Y., Boyd, C. M., Klein, M., Bougiatioti, A., Cerully, K. M., Hite, J. R., Isaacman-VanWertz, G., Kreisberg, N. M., Knote, C., Olson, K., Koss, A., Goldstein, A. H., Hering, S. V., de Gouw, J., Baumann, K., Lee, S. H., Nenes, A., Weber, R. J., and Ng, N. L.: Effects of anthropogenic emissions on aerosol formation from isoprene and monoterpenes in the southeastern United States, *Proc. Nat. Acad. Sci. U.S.A.*, 112, 37-42, 10.1073/pnas.1417609112, 2015.

Xu, Z. N., Nie, W., Liu, Y. L., Sun, P., Huang, D. D., Yan, C., Krechmer, J., Ye, P. L., Xu, Z., Qi, X. M., Zhu, C. J., Li, Y. Y., Wang, T. Y., Wang, L., Huang, X., Tang, R. Z., Guo, S., Xiu, G. L., Fu, Q. Y., Worsnop, D., Chi, X. G., and Ding, A. J.: Multifunctional Products of Isoprene Oxidation in Polluted Atmosphere and Their Contribution to SOA, 48, e2020GL089276, <https://doi.org/10.1029/2020GL089276>, 2021.

Yan, C., Nie, W., Aijala, M., Rissanen, M. P., Canagaratna, M. R., Massoli, P., Junninen, H., Jokinen, T., Sarnela, N., Hame, S. A. K., Schobesberger, S., Canonaco, F., Yao, L., Prevot, A. S. H., Petaja, T., Kulmala, M., Sipila, M., Worsnop, D. R., and Ehn, M.: Source characterization of highly oxidized multifunctional compounds in a boreal forest environment using positive matrix factorization, *Atmos. Chem. Phys.*, 16, 12715-12731, 10.5194/acp-16-12715-2016, 2016.

Yan, C., Nie, W., Vogel, A. L., Dada, L., Lehtipalo, K., Stolzenburg, D., Wagner, R., Rissanen, M. P., Xiao, M., Ahonen, L., Fischer, L., Rose, C., Bianchi, F., Gordon, H., Simon, M., Heinritzi, M., Garmash, O., Roldin, P., Dias, A., Ye, P., Hofbauer, V., Amorim, A., Bauer, P. S., Bergen, A., Bernhammer, A. K., Breitenlechner, M., Brilke, S., Buchholz, A., Mazon, S. B., Canagaratna, M. R., Chen, X., Ding, A., Dommen, J., Draper, D. C., Duplissy, J., Frege, C., Heyn, C., Guida, R., Hakala, J., Heikkinen, L., Hoyle, C. R., Jokinen, T., Kangasluoma, J., Kirkby, J., Kontkanen, J., Kurten, A., Lawler, M. J., Mai, H., Mathot, S., Mauldin, R. L., Molteni, U., Nichman, L., Nieminen, T., Nowak, J., Ojdanic, A., Onnela, A., Pajunoja, A., Petaja, T., Piel, F., Quelever, L. L. J., Sarnela, N., Schallhart, S., Sengupta, K., Sipila, M., Tome, A., Trostl, J., Vaisanen, O., Wagner, A. C., Ylisirnio, A., Zha, Q., Baltensperger, U., Carslaw, K. S., Curtius, J., Flagan, R. C., Hansel, A., Riipinen, I., Smith, J. N., Virtanen, A., Winkler, P. M., Donahue, N. M., Kerminen, V. M., Kulmala, M., Ehn, M., and Worsnop, D. R.: Size-dependent influence of NO_x on the growth rates of organic aerosol particles, *Science Advances*, 6, 9, 10.1126/sciadv.aay4945, 2020.

Zhao, D. F., Buchholz, A., Kortner, B., Schlag, P., Rubach, F., Kiendler-Scharr, A., Tillmann, R., Wahner, A., Flores, J. M., Rudich, Y., Watne, Å. K., Hallquist, M., Wildt, J., and Mentel, T. F.: Size-dependent hygroscopicity parameter (κ) and chemical composition of secondary organic cloud condensation nuclei, *Geophys. Res. Lett.*, 42, 10920-10928, 10.1002/2015gl066497, 2015a.

Zhao, D. F., Kaminski, M., Schlag, P., Fuchs, H., Acir, I. H., Bohn, B., Häsel, R., Kiendler-Scharr, A., Rohrer, F., Tillmann, R., Wang, M. J., Wegener, R., Wildt, J., Wahner, A., and Mentel, T. F.: Secondary organic aerosol formation from hydroxyl radical oxidation and ozonolysis of monoterpenes, *Atmos. Chem. Phys.*, 15, 991-1012, 10.5194/acp-15-991-2015, 2015b.

Zhao, D. F., Schmitt, S. H., Wang, M. J., Acir, I. H., Tillmann, R., Tan, Z. F., Novelli, A., Fuchs, H., Pullinen, I., Wegener, R., Rohrer, F., Wildt, J., Kiendler-Scharr, A., Wahner, A., and Mentel, T. F.: Effects of NO_x and SO₂ on the secondary organic aerosol formation from photooxidation of alpha-pinene and limonene, *Atmos. Chem. Phys.*, 18, 1611-1628, 10.5194/acp-18-1611-2018, 2018.

Ziemann, P. J., and Atkinson, R.: Kinetics, products, and mechanisms of secondary organic aerosol formation, *Chem. Soc. Rev.*, 41, 6582-6605, 10.1039/c2cs35122f, 2012.